Reviewer#1

In this manuscript, Yuan et al. proposed two new methods for estimating isotope ratio of background air vapor (delta_a) based on data collected from standard keeling-plot setups. The study is timely given that delta_a is an important variable that can yield insights into certain aspects of water cycling, but nonetheless remains underexplored as its estimation is not possible with the traditional keeling plot approach. After going through the manuscript, I feel that both of the proposed methods are interesting, theoretically well-grounded and based upon realistic assumptions. Nevertheless, I have some comments that may be of help for strengthening this manuscript, as the following.

Response: We thank the referee for the positive feedbacks.

Although the theoretical framework underlying the IP method is sufficiently sound, I feel that the authors' presentation of this method lacks clarity in several aspects. For example, one thing that I don't fully understand is why the method was named as the "intersection point" method in the first place. I understand that the proposed method was based on Yamanaka and Shimizu (2007) in which delta_a was estimated through the y (or delta_v) value of the point at which two keeling-plot lines intersect. However, it is clear from Equations 4 and 5 (L108, L109) that the method is based on a regular procedure of solving two equations for two unknowns, and that it actually does not have much to do with calculating an intersect point (this typically would involve calculation of a x (or 1/cv) value that would render equality between two y (or delta_v) values predicted from the two different keeling plots). So maybe a different name should be used to describe this method, so to represent the underlying mathematical mechanism more accurately. Further, the so-called IP method was developed with a vertical-profile based keeling plot as a context, but it is unclear to me what data should be used for parameterizing Cv1, Cv2, delta_v1, and delta_v2 in order for calculating delta_a from Eqn.6 (L112). For example, would the authors recommend parameterizing Cv1 using vapor concentration measured at a particular height at t1? If yes then which level of height would you prefer to use and why?

Response: We are grateful for the constructive comments from the reviewer. We provided detailed explanations in the following.

Strictly speaking, if delta_a is estimated from Eqn. 6 based on vapor concentration and isotope measurements at a particular height, then the resultant delta_a could be inevitably subject to some error the degree of which may likely depend on how much the difference (or the residual not explained by the regression equation) exists between the measured concentration value (i.e. Cv1) at this height and that predicted from the keeling plot (i.e. the regression line derived from measurements from all heights). To reduce this estimation error, I would suggest that the following calculation equations be used instead:

Ca(delta_a – delta_ET1) = k1 (Eqn.1)

Ca(delta_a – delta_ET2) = k2 (Eqn.2)

Where k1 and delta_ET1 denote values for KP1 (keeling plot at time 1) derived slope and intercept respectively, and k2 and delta_ET2 correspond to KP2 derived values. Combining Eqns. 1 and 2 yields an equation for calculating delta_a, as:

delta_a = (k2*delta_ET1 – k1*delta_ET2)/(k2 – k1) (Eqn. 3)

The eqn.3 shown above may be more advantageous than the originally presented Eqn. 6, due to that it is simpler in structure, and does not require isotope measurement at a particular height.

Response: We are grateful for the constructive comments from the reviewer. We apologize that we mistakenly thought that the original Eq. 4 and 5 were able to represent the process that δ_a was estimated through the y (or δ_v) value of the point at which two Keeling-plot lines intersect. In fact, the result of IP method was exactly based on intersection point of two adjacent moments Keeling plots. That was the reason why we called it "intersection point" method. Original Eq. 4 and 5 were not used in the actual calculations. We revised the IP method description as suggested. The following is our newly added description of IP method. Since the actual calculations in the original manuscript followed the revised procedure, there are no changes in our results.

"**Intersection point (IP) method**. Note that for two nearby time points t_1 and t_2, we could use local constant approximation to estimate δ_a within this time interval since it remains relatively constant over a short period of time. By assuming local constant for C_a and δ_a within this time interval, we have

$$k_1 = C_a(\delta_a - \delta_{ET_1}) \quad , \qquad (4)$$

$$k_2 = C_a(\delta_a - \delta_{ET_2}) \quad , \qquad (5)$$

where k_i and δ_{ET_i} represent the value at t_i for i=1, 2. From (4) and (5), we can solve δ_a as:

$$\delta_a = \frac{k_1\delta_{ET_2} - k_2\delta_{ET_1}}{k_1 - k_2} \quad . \qquad (6)$$

The local constant approximation idea was first described in Yamanaka and Shimizu (2007) as an assumption to quantify the contribution of local ET to total atmospheric vapor. "

It seemed that the new Eq. 4 and 5 had nothing to do with C_v and δ_v. However, δ_{ET_1} and δ_{ET_2} were estimated by clastic Keeling plots, which replied on C_v and δ_v measurements from all eight heights.

More specific comments as below:

L36: change "replying" to "relying"

Response: Corrected.

L45: Maybe I missed it, but I did not see anywhere in the text that evidence is presented to support the constant delta_a assumption. A possible route that I could image towards proof of this concept would be to first use Eqns. 6 or 7 to calculate delta_a at different heights using height-specific Cv and delta_v measurements. However, these calculations would have to be based on keeling plot derived delta_ET values, and thus already involve assuming that delta_a remains constant across different heights. In other words, the constant delta_a assumption is already a prerequisite for performing calculation of delta_a, and so one would easily fall into the trap of circular reasoning if the calculated delta_a values are further used as a test of the constant delta_a assumption.

Response: We thank the reviewer for pointing this out and we apologize for the oversight. The reviewer is correct, we did not show evidence in the text to support the constant δ_a assumption. We just used this assumption in our study. We deleted the related description to correct this oversight and avoid confusion.

L57-60: This sentence reads awkward and requires some re-writing. i.e., may be better off beginning the sentence with something like: "With the advent of laser isotope spectrometry capable of continuous and high-frequency measurements of...."

L60-61: Same as above. May be re-organized into something like: "the number of studies...was continuously increasing, generating new insights into processes that affect dv."

Response: We revised this sentence as suggested and altered the order.

"With the advent of laser isotope spectrometry capable of high frequency (1 Hz) measurements of the isotopic composition of atmospheric water vapor (δ_v) and atmospheric water vapor content (C_v) (Kerstel and Gianfrani, 2008; Wang et al., 2009), the number of studies based on high frequency ground-level isotope measurements was continuously increasing. These studies generate new insights into the processes that affect δ_v, including meteorological factors (Galewsky et al., 2011; Steen-Larsen et al., 2013), biotic factors (Wang et al., 2010) and multiple factors (Parkes et al., 2016). Such increase in δ_v measurements allows an isotope-enabled global circulation models (Iso-GCMs) to estimate the variation of water vapor isotope parameters at a global scale (Werner et al., 2011). Concomitantly, more than δ_v, several new methods using high frequency ground-level isotope measurements were devised to directly estimate the isotopic composition of leaf water (Song et al., 2015) and leaf transpired vapor (Wang et al., 2012)."

Parkes, S., McCabe, M., Griffiths, A. D., Wang, L., Chambers, S., Ershadi, A., Williams, A. G., Strauss, J., and Element, A.: Response of water vapour D-excess to land-atmosphere interactions in a semi-arid environment, **Hydrology and Earth System Sciences**, 21, 533–548, doi:10.5194/hess-21-533-2017, 2016.

Song, X., Simonin, K. A., Loucos, K. E., and Barbour, M. M.: Modelling non-steady-state isotope enrichment of leaf water in a gas-exchange cuvette environment, **Plant, Cell & Environment**, 38, 2618-2628, doi: 10.1111/pce.12571, 2015.

Wang, L., Caylor, K. K., Villegas, J. C., Barron-Gafford, G. A., Breshears, D. D., and Huxman, T. E.: Partitioning evapotranspiration across gradients of woody plant cover: Assessment of a stable isotope technique, **Geophysical Research Letters**, 37, L09401, doi: 10.1029/2010GL043228, 2010.

Wang, L., Good, S. P., Caylor, K. K., and Cernusak, L. A.: Direct quantification of leaf transpiration isotopic composition, **Agricultural and Forest Meteorology**, 154-155, 127-135, doi: 10.1016/j.agrformet.2011.10.018, 2012.

Werner, M., Langebroek, P. M., Carlsen, T., Herold, M., and Lohmann, G.: Stable water isotopes in the ECHAM5 general circulation model: Toward high-resolution isotope modeling on a global scale, **Journal of Geophysical Research: Atmospheres**, 116, D15109, doi:10.1029/2011JD015681, 2011.

L76-78: I would suggest that the authors add one or two sentences here to highlight why delta_a is important, or how and why accurate estimation of delta_a would benefit ecohydrolgocial studies.

Response: We thank the reviewer for the constructive comment. As suggested, we added more information below about how and why accurate estimation of δ_a would benefit ecohydrolgocial studies.

"ET is a crucial component of water budget across scales such as field (Wagle et al., 2020), watershed (Zhang et al., 2001), regional (Hobbins et al., 2001) and global (Jung et al., 2010) scales. The water isotopic composition of ET (δ_{ET}) was generally estimated by Keeling plot approach (Keeling, 1958). It was first used to explain carbon isotope ratios of atmosphere CO_2 and to identify the sources that contribute to increases in atmospheric CO_2 concentration, and has been further used to estimate δ_{ET} in recent two decades (Yakir and Sternberg, 2000). Keeling plot analyses can be applied using δ_v and C_v output by laser based analyzer either from different heights (Yepez et al., 2003; Zhang et al., 2011; Good et al., 2012) or at one height with continuous observations (Wei et al., 2015; Keppler et al., 2016). Although the intercept of the linear regression line was commonly used as estimated δ_{ET}, the slope of the Keeling plot was also used to estimate δ_{ET} by re-arranging the Keeling plot equations (Miller and Tans, 2003; Fiorella et al., 2018). Keeling plot approach was based on isotope mass balance and two-source assumption using two equations with three unknowns. As a result, the isotopic composition of other potential sources (e.g., water vapor not from ET), as well as isotopic composition of ambient water vapor (δ_a), were not able to be estimated directly using the Keeling plot approach. That is one of the reasons why field scale moisture recycling is difficult to estimate to date."

Hobbins, M. T., Ramirez, J. A., and Brown, T. C.: The complementary relationship in estimation of regional evapotranspiration: An enhanced advection-aridity model, **Water Resources Research**, 37, 1389-1403, doi: 10.1029/2000WR900359, 2001.

Jung, M., Reichstein, M., Ciais, P., Seneviratne, S. I., Sheffield, J., Goulden, M. L., Bonan, G., Cescatti, A., Chen, J., and De Jeu, R.: Recent decline in the global land evapotranspiration trend due to limited moisture supply, **Nature**, 467, 951-954, doi: 10.1038/nature09396, 2010.

Wagle, P., Skaggs, T. H., Gowda, P. H., Northup, B. K., and Neel, J. P.: Flux variance similarity-based partitioning of evapotranspiration over a rainfed alfalfa field using high frequency eddy covariance data, **Agricultural and Forest Meteorology**, 285, 107907, doi: 10.1016/j.agrformet.2020.107907, 2020.

Zhang, L., Dawes, W., and Walker, G.: Response of mean annual evapotranspiration to vegetation changes at catchment scale, **Water Resources Research**, 37, 701-708, doi: 10.1029/2000WR900325, 2001.

L106: "it is changing smoothly over time" – maybe change into sth like "it remains relatively constant over a short period of time"?

Response: Changed as suggested.

L152: change "isotope and gas concentration analyzer" to "water vapor isotope analyzer".

Response: Corrected.

L236/238: "immediate intermediate theorem" – no need to spell out the full name here, can just replace with IVT.

Response: Changed as suggested.

L276: What about arid ecosystem? Which method would you recommend for use? From what I understand, the IVT method may also be less favored, due to that it relies on more stringent criteria for data filtering (meaning higher percentage of data loss?), but I could also have missed some strengths/advantages related to this method. Further, can these two methods also be extended to time-based keeling plot cases? Maybe some additional discussion on these topics would be helpful.

Response: We thank the reviewer for the constructive comment. We overlooked the comparation of two methods. The IP method has a wide applicability among various ecosystem and has less constraining data criteria, while IVT method requires less parameters to estimate δ_a. The following is the newly added.

"It also reflected that IVT method could only be used in non-arid ecosystems to ensure the appearance of Keeling plot slope sign switch. On the contrary, IP method may not be restricted by the type of ecosystems."

L280: Your method is similar to Y&Z (2007) in that both require two keeling plot-based equations for solving for two unknowns. However, the two methods are not entirely the same, as for your method, the two unknowns to be solved are delta_a and Ca (having little to do with an intersection point), whereas for Y&Z, the two unknowns to be solved are delta_v and Cv, with the resolved delta_v considered the same as delta_a because of the meaning imbedded within an intersection point.

Response: We thank the reviewer for the constructive comment. We apologize for our oversight for the expression of Eq. (4) and (5). In reality, IP method also had two unknowns (C_v and δ_v) to be solved. We think Y&Z's method was spatial based. They assumed local constant C_a and δ_a within nearby sites. However, IP method in our study was temporal based. We assumed local constant for C_a and δ_a within 30-minute time interval.

L287: change "is consisted of" to "consists of"

Response: Corrected.

L303: See my previous comment on L45.

Response: Please refer to our response to L45 and the same changes have been implemented.

Reviewer#2

The manuscript "Novel Keeling plot based methods to estimate the isotopic composition of ambient water vapor" presents two methods to use existing Keeling plot data not only to calculate the isotopic composition of a source (here ET), but also that of ambient water vapor delta_a. Using these two methods might provide new insights into the variability of delta_a, but a rigorous evaluation and discussion of the limitations and biases of these methods would be needed.

I cannot recommend publication of the submitted manuscript in this form. The paper lacks detailed and clear descriptions of methods and evaluation steps in many points. Due to the small number of data points that fulfilled the quality criteria, it is not clear which significance the results have and if the strong conclusions of the manuscript are justified.

Response: We thank the reviewer for the insightful and critical comments. Addressing these comments certainly improved the quality of our manuscript. We made thorough changes through expanding the field data set, adding more descriptions of the methods and evaluation procedures as well as providing more details of the theoretical derivations. More details are in the sections bellow.

In particular I am worried about the following points:

The sparsity of the data is a major problem of the submitted manuscript. Out of four months of data, only 4 days were used for data evaluation.

Response: We thank the reviewer for the constructive comment. Our goal is to provide two new methods to estimate a parameter that is rarely estimated or measured in the past. Our key contribution of this study is the theoretical derivation of the two new methods and the data evaluation component is less important. However, we agree more field data evaluation will strengthen the manuscript. As such, we expanded our database from 4 days to 49 days including all the possible field observations during May to September, 2017 to evaluate the two methods.

Further, many data points had to be removed because they produced contradictions with the assumption. (line 197 ff). If both methods produce so many data points that are obviously wrong, it is not clear to me why we should trust the other data points. At least it needs a detailed discussion why there are roughly 50% respectively 80% of obviously wrong values. Is the used data set inaccurate and/or are limitations of the methods producing these values? Are we sure that these problems do not occur for the remaining data points?

Response: Thanks for the comments. We think the expression of "XX% of δ_a values were acceptable" generates some confusion. With 30-min interval in 49 days, we should have gotten 2352 δ_a values. However, with a precondition $k_1k_2<0$ for IVT method and a filter ($\delta_{ET}<\delta_v<\delta_a$ or $\delta_{ET}>\delta_v>\delta_a$) for both methods, some of the field observations do not meet the criteria. We added a new **Table 1** here to provide more details. The total δ_a is 48 for each day as each 30-minute interval should have one δ_a value. However, we do not have 48 usable δ_a for most days. On May 19th, for instance, the number of $\delta_{a(IP)}$ and $\delta_{a(IVT)}$ values passing the filter ($\delta_{ET}<\delta_v<\delta_a$ or $\delta_{ET}>\delta_v>\delta_a$) are 27 and 8, respectively. After the expansion of field observations, there are 53.8% and 4.8% of δ_a values meeting the criteria using IP and IVT method, respectively. We think the δ_a values deviating the criteria does not mean "wrong values". For one thing, if the filter is not applied, 100% of $\delta_{a(IP)}$ and 5.8% of $\delta_{a(IVT)}$ is acceptable. The low percentage of $\delta_{a(IVT)}$ meeting the criteria is mainly because only 5.8% of the 30-min intervals obey the precondition of $k_1k_2<0$. For another, if the filter is not applied, the linear regression between $\delta_{a(IP)}$ and $\delta_{a(IVT)}$ is still significant ($\delta_{a(IP)} = 0.9975\delta_{a(IVT)} - 0.0425$, $R^2 = 0.9959$, $p<0.001$, $n=150$). In fact, the filter ($\delta_{ET}<\delta_v<\delta_a$ or $\delta_{ET}>\delta_v>\delta_a$) is necessary for further calculation (e.g., C_{ET} and f_{ET} in line 245-246) rather than an assumption of our methods. We made these clearer in the revision.

Table 1. The number of estimated isotope composition of ambient vapor meeting the criteria using the intersection point method ($\delta_{a(IP)}$) and the Intermediate Value Theorem method ($\delta_{a(IVT)}$) among all 49 days.

Date	number of $\delta_{a\ (IP)}$ values meeting the criteria in a whole day	number of $\delta_{a\ (IVT)}$ values meeting the criteria in a whole day
5/19	27	8
5/27	13	3
5/28	30	3
5/31	25	5
6/4	38	5
6/5	28	0
6/7	29	6
6/9	32	5
6/10	26	2
6/11	21	4
6/12	22	4
6/15	32	0
6/16	33	0
6/17	24	1
6/18	26	0
6/21	26	3
6/22	22	0
6/26	22	0
6/27	29	3
7/4	23	0
7/5	23	1
7/7	30	0
7/8	29	0
7/14	28	4
7/16	28	0
7/18	25	1
7/19	28	6
7/20	27	6
7/21	29	0
7/22	19	0
8/3	18	1
8/4	22	3
8/5	25	3
8/6	28	1
8/12	13	8
8/18	19	3
8/19	30	0
8/28	23	0
8/29	22	1
8/30	27	1
8/31	27	0
9/20	25	0
9/21	24	1
9/22	31	1
9/23	28	1
9/27	28	2
9/28	25	1
9/29	30	5
9/30	25	1

The conclusion in line 39 (consistency between results and HYSPLIT modelling) and the statement in line 235 ff ("The calculated delta_a values on 11th June and 12th August ... were higher than on the other days") is not very well supported by the data. Firstly, there are only four data points. Secondly, the data is not that clear for the IP method: In line 204 it is written that the values were -12.95permil on 19th of May and -12.77permil on 12th of August. This is a difference of only approximately 0.2 permil. As there are so few data points for the comparison to modelling, the conclusion in line 39 is far to strong.

Response: We thank the reviewer for the constructive comment. Instead of using four representative days, we utilized all 49 days in this revision but made quality controls. After we expanded the database, we made a new time series of isotopic variation (**Fig. 2**) to replace the original **Fig. 2**. To ensure the representativeness of diurnal average $\delta_{a(IVT)}$, we removed 28 of 49 days (**Table 1**) because the number of acceptable $\delta_{a(IVT)}$ is no more than one in these 28 days. After this kind of quality control, we made two new figures (**Fig. 3a** and **Fig. 3b**). Fig. 3a shows external origins and **Fig. 3b** shows local origins based on HYSPLIT. Almost all of the $\delta_{a(IP)}$ and $\delta_{a(IVT)}$ in **Fig. 3a** is smaller than that of **Fig. 3b**.

"The 500 m height water vapor backward trajectories revealed that water vapor was from outside the study regions for ten days (**Fig. 3a**), and water vapor was from local ET for eight days (**Fig. 3b**)."

"As for the IP method, 53.7% of $\delta_{a(IP)}$ values met the criteria, and 49.4% of $\delta_{a(IP)}$ values meeting the criteria were during the daytime (7:00am-7:00pm). The range of $\delta_{a(IP)}$ values meeting the criteria were between -16.79‰ and -12.95‰ for the ten days with external origins (**Fig. 3a**). The range of $\delta_{a(IP)}$ values meeting the criteria were between -12.77‰ and -9.51‰ for the eight days with local origins (**Fig. 3b**)."

"As for the IVT method, only 4.4% of δ_a values met the criteria, and 35.9% of δ_a values meeting the criteria were during the daytime (7:00am-7:00pm). The range of $\delta_{a(IVT)}$ values meeting the criteria were between -16.31‰ and -13.93‰ for the ten days with external origins (**Fig. 3a**). The range of $\delta_{a(IVT)}$ values meeting the criteria were between -12.67‰ and -9.12‰ for the eight days with local origins (**Fig. 3b**)"

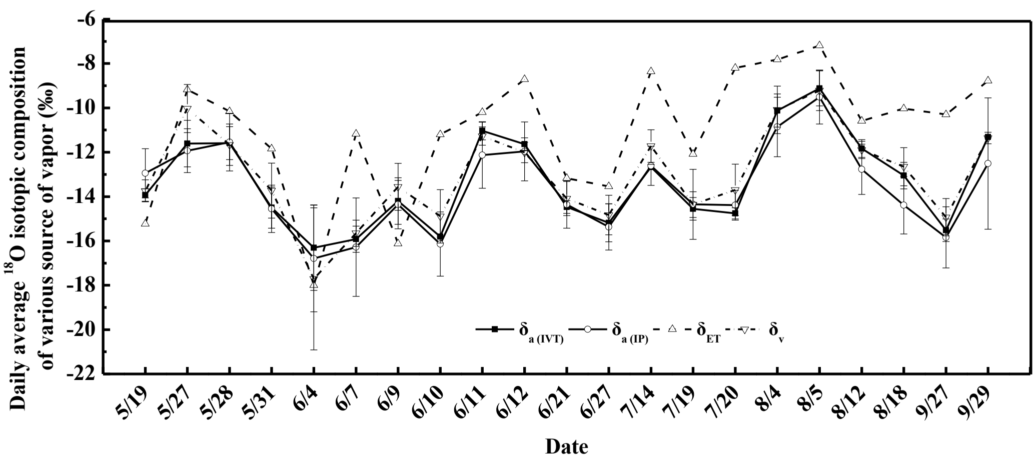

Fig. 2 The daily average values of the isotope composition of evapotranspiration vapor (δ_{ET}), the isotope composition of atmospheric vapor (δ_v), the estimated isotope composition of ambient vapor using the intersection point method ($\delta_{a(IP)}$) and the Intermediate Value Theorem method ($\delta_{a(IVT)}$) in all 49 days.

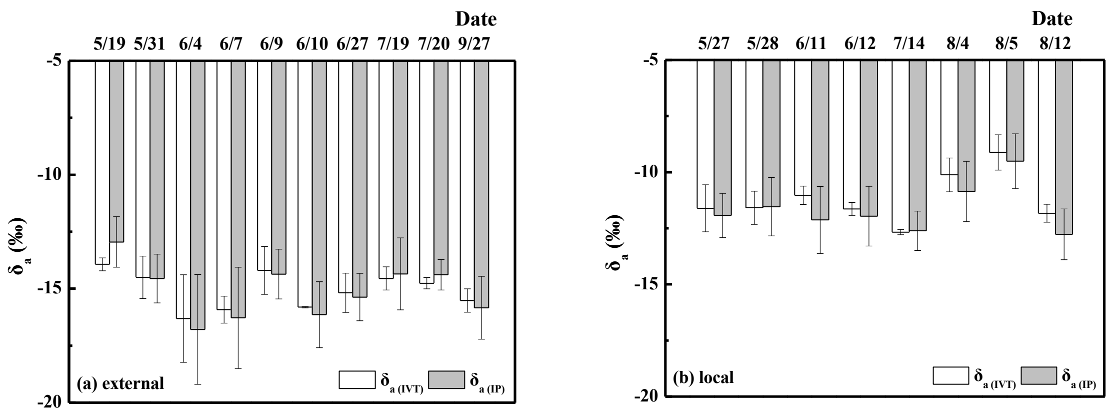

Fig. 3 The daily average values of the estimated isotope composition of ambient vapor using the intersection point method ($\delta_{a(IP)}$) and the Intermediate Value Theorem method ($\delta_{a(IVT)}$) after filter. Hybrid Single Particle Lagrangian Integrated Trajectory (HYSPLIT) backward trajectory showed external origin (a) and local origin (b), respectively.

The diurnal averages of the methods (lines 202ff and line209ff) are quite different between the two models (up to 1 permil but in both directions). The difference between day and night values is app. -1.6 permil for the IP method and 0.02 permil for the IVT method (lines 205 and 211 resp.) Thus, on a daily scale, the method comparison (Fig. 4) is much worse than on a point to point scale. Without providing a time series, it is hard to understand what is the problem here and to see e.g. in how far the diurnal means are uncertain and contain more or less data points. Thus, the conclusion in line 239 is not very well supported by the data.

Response: We thank the reviewer for the constructive comment. We added new **Fig. 4** in the revision to address these comments. After we expanded the database, the method comparison at daily scale (**Fig. 4a**) is still not as good as the point to point scale (**Fig. 4b**). This is mainly because the number of acceptable $\delta_{a(IP)}$ is far more than that of acceptable $\delta_{a(IVT)}$ for the point to point scale due to the precondition of IVT method ($k_1k_2<0$). As such, the daily results for $\delta_{a(IP)}$ and $\delta_{a(IVT)}$ are based on different numbers of data points. We revised the conclusion in line 239 as follow.

"The reliability of two methods at point to point scale were also supported by the close relationship of δ_a using these two independent methods. Daily time scale result is less reliable than point to point scale."

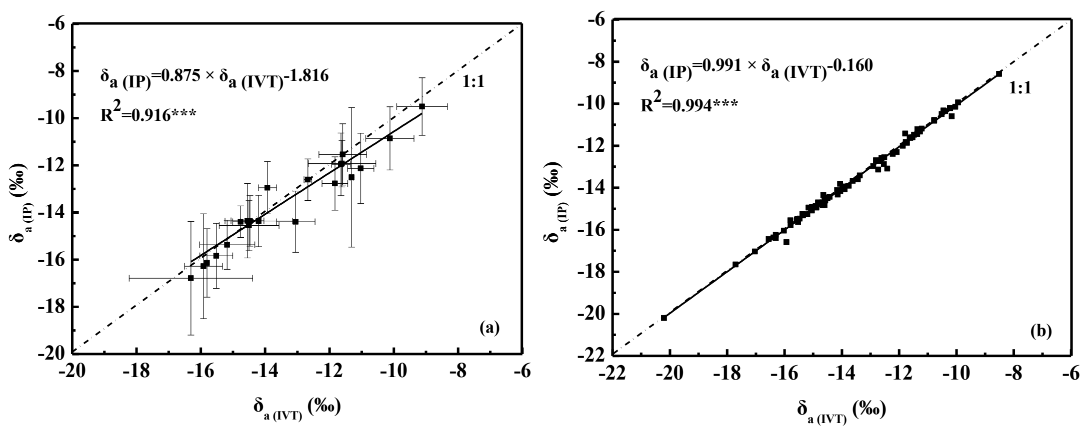

Fig. 4 Linear regression between the estimated isotope composition of ambient vapor using the intersection point method ($\delta_{a(IP)}$) and the Intermediate Value Theorem method ($\delta_{a(IVT)}$) on daily scale (a) and point to point scale (b), respectively

The manuscript generally lacks a careful discussion of the (propagated) uncertainties and limitations of both methods as well as of the used data (e.g. Fig. 4 is without errorbars)

Response: Thanks for the comment. We added more discussion of the uncertainty and limitations in the revised manuscript. In the revision, we also added error bars on daily scale method comparison (**Fig. 4a**) and time series of δ_{ET}, δ_v, $\delta_{a(IP)}$ and $\delta_{a(IVT)}$ from May to September (**Fig. 2**).

Throughout the manuscript, there are many unclearities/missing details that makes it hard for the reader to understand what has been done and makes it hard to assess the results. For many of these points it might indeed help to use more references.

Response: Thanks for the comment. We thoroughly revised the materials & method part and results part. More details are shown in the following responses.

In the methods section, there is barely no detail about the calculation of the Keeling plots such as the following: How many data points were used for one Keeling plot calculation? Which data points were used (spatial and temporal) in a single Keeling plot)? Was the calibration procedure a) a standard procedure that has been used elsewhere (if so, please provide a reference) or b) carefully evaluated?

Response: Thanks for the comment. As was shown in the materials and methods section, one Keeling plot calculation contained eight heights of δ_v and C_v (line152). The eight heights data was collected in 30 mins (line165-line166). Therefore, a single Keeling plot considered eight different heights in one time point (line 101). The calibration procedure was a standard procedure that had been used. Our calibration procedure mainly referred to the study by Steen-Larsen et al. (2013). In their study, six steps of calibration protocols were provided in 2.4 section. The calibration protocols were followed in our study. Moreover, we had some different measures to fit our study, which were carefully evaluated. For example, compared with their 15-min-interval switch of different heights, our study shortened this interval into 225s to ensure a relative stable value of δ_a, C_a and C_{ET}. Data from No. 195 to No. 253 was used. The absolute value of coefficient of variations (|CV|) of δ_v and C_v were no more than 0.016 and 0.002, respectively, which was far below the critical value of 15% (Lovie, 2005). C_v gradients calibration was the third calibration step in Steen-Larsen et al. (2013). We made some revise on this part.

"Our calibration procedure mainly followed the study by Steen-Larsen et al. (2013) with some modifications to fit our specific experimental setup. The water vapor from eight inlets were sampled continuously over a 24-hour-period. Since only one analyzer was used to measure the δ_v and C_v, the values of eight sampling inlets were recorded in turn every 225s in a 30 mins cycle. The switch procedure was automatic. As the analyzer makes a measurement every 0.9-1s, approximately 259-264 values for each inlet was recorded within the cycle. For each 225s measurement period, No. 195 to No. 253 data points were used to avoid memory issue and influence of transient pressure variation. The absolute value of coefficient of variations (|CV|) of δ_v and C_v were no more than 0.016 and 0.002, respectively, which was far below the critical value of 15% (Lovie, 2005). The mean value of the selected data points was regarded as the measured δ_v and C_v in a specific inlet. Measured C_v was used directly as actual C_v, while measured δ_v was calibrated to minimize the influence of isotopic concentration dependence. The C_v in our measurement ranged from 5386 ppm to 30255 ppm. Thus, C_v gradients of 10000 ppm, 20000 ppm and 30000 ppm were selected as calibration concentrations to improve the precision of δ_v."

Lovie, P.: Coefficient of variation, **Encyclopedia of statistics in behavioral science**, doi: 10.1002/0470013192.bsa107, 2005.

Steen-Larsen, H. C., Johnsen, S. J., Masson-Delmotte, V., Stenni, B., Risi, C., Sodemann, H., Balslev-Clausen, D., Blunier, T., Dahl-Jensen, D., and Ellehøj, M. D.: Continuous monitoring of summer surface water vapor isotopic composition above the Greenland Ice Sheet, **Atmospheric Chemistry and Physics**, 13, 4815-4828, doi: 10.3929/ethz-b-000067919, 2013.

For the IP method, there are more details needed such as: What is the time step between the two Keeling plots that are used? Which of them are used as delta_v and c_v? If all of them are used, you get 8 different delta_a from one single Keeling plot. What did you do with them? Are they treated as individual measurements or are they averaged or did you pick one of them?

Response: We are grateful for the constructive comments from the reviewer. We apologize that we mistakenly thought that the original Eq. 4 and 5 were able to represent the process that δ_a was estimated through the y (or δ_v) value of the point at which two Keeling-plot lines intersect. In fact, the result of IP method was exactly based on intersection point adjacent moments of two Keeling Plots. That was the reason why we call it "intersection point" method. Original Eq. 4 and 5 were not used in the actual calculations. We revised the IP method description. The following is our newly added description of IP method. Since the actual calculations in the original manuscript followed the revised procedure, there are no changes in our results.

"**Intersection point method**. Note that for two nearby time points t_1 and t_2, we could use local constant approximation to estimate δ_a within this time interval since it remains relatively constant over a short period of time. By assuming local constant for C_a and δ_a within this time interval, we have

$$k_1 = C_a(\delta_a - \delta_{ET_1}) \quad , \qquad (4)$$

$$k_2 = C_a(\delta_a - \delta_{ET_2}) \quad , \qquad (5)$$

where k_i and δ_{ET_i} represent the value at t_i for i=1, 2. From (4) and (5), we can solve δ_a as:

$$\delta_a = \frac{k_1\delta_{ET_2} - k_2\delta_{ET_1}}{k_1 - k_2} \quad . \qquad (6)$$

The local constant approximation idea was first described in Yamanaka and Shimizu (2007) as an assumption to quantify the contribution of local ET to total atmospheric vapor. "

It seemed that the new Eq. 4 and 5 had nothing to do with C_v and δ_v. However, δ_{ET_1} and δ_{ET_2} were estimated by clastic Keeling plots, which replied on C_v and δ_v from all eight heights.

Yamanaka, T., and Shimizu, R.: Spatial distribution of deuterium in atmospheric water vapor: Diagnosing sources and the mixing of atmospheric moisture, **Geochimica et cosmochimica acta**, 71, 3162-3169, doi: 10.1016/j.gca.2007.04.014, 2007.

In the conclusion, it is written "The results show an evidence that delta_a was constant ... among different heights". I would like to see the data on which this conclusion is based.

Response: We thank the reviewer for the constructive comment. We did not show any evidence in the text to support the constant δ_a assumption. We just used this assumption in our study. We deleted the related description and apologize for the oversight.

Please provide a time series of all results and indicate the 14 points used for the comparison. The boxplots in Figure 1 can hide interesting features of delta_a. A time series would help to discuss potential problems of the methods e.g. to test the assumption that delta_a is constant at a sufficient timescale.

Response: We thank the reviewer for the constructive comment. After we expanded the database, a time series of all results are shown in **Fig. 2**. Standard deviation (Std) values were selected here to evaluate the constancy among isotopic parameters at daily scale. Std(δ_{ET}), Std(δ_v), Std($\delta_{a(IP)}$) and Std($\delta_{a(IVT)}$) were 6.08, 0.91, 1.38 and 0.59, respectively. As a result, the constancy of δ_a was similar to the constancy of δ_v at daily scale. We added a time series of all results in the results part.

"Time series of isotopic variations were shown in **Fig. 2**. The δ_v here is the average value of eight heights. The average δ_{ET}, δ_v, $\delta_{a(IP)}$ and $\delta_{a(IVT)}$ were -11.04‰, -13.00‰, -13.60‰ and -13.29‰, respectively in those 21 days when more than one $\delta_{a(IVT)}$ was attained for each day. Daytime (7:00am-7:00pm) average δ_{ET}, δ_v, $\delta_{a(IP)}$ and $\delta_{a(IVT)}$ were -10.73‰, -13.33‰, -14.08‰ and -13.63‰, respectively. While at nighttime (7:00pm-7:00am the next day), average δ_{ET} was lower than that at daytime, which was on the contrary with δ_v, $\delta_{a(IP)}$ and $\delta_{a(IVT)}$. The trend of $\delta_{a(IP)}$ and $\delta_{a(IVT)}$ were similar to δ_v. In majority of circumstances, δ_{ET} is the largest of those four isotopic parameters, except on May 19th, June 4th and June 9th. About 76% of k values were negative, and most positive k values occurred at nighttime (60%). The percentage of positive k values were 33%, 34%, 24%, 34% and 10% in May, June, July, August and September, respectively. Standard deviation was used here to evaluate the constancy among isotopic parameters at daily scale. The standard deviation of δ_{ET}, δ_v, $\delta_{a(IP)}$ and $\delta_{a(IVT)}$ were 6.08‰, 0.91‰, 1.38‰ and 0.59‰, respectively. Therefore, the constancy of δ_a was similar to the constancy of δ_v at daily scale."

The results are presented as showing "four typical days" without any indication how the term "typical" is used here and in particular no data driven evidence for the claim that there four days are "typical".

Response: Thanks for the comment. We have expanded the database as suggested and abandoned the term "typical".

In Fig 4, there is no statistics given on the deviation between these models - such as sqrt(mean(delta_IP - delta_IVT)2)). This would give helpful additional information. Additionally, slope and Offset of the regression line in Fig. 4 could be discussed separately. Thus, there seems to be an offset of 0.748 between the two methods. Please discuss this offset.

Response: Thanks for the comment. The sqrt(mean($(\delta_{a(IP)}-\delta_{a(IVT)})^2$)) between these two methods on daily scale and point to point scale were 0.618‰ and 0.167‰, respectively. This indicated that two methods were well matched on point to point scale. The slope and offset of point to point scale regression were closer to one than that of daily scale. As IVT method rely on an approximate valuation of $\delta_a \in [min(\delta_{v_1}, \delta_{v_2}), max(\delta_{v_1}, \delta_{v_2})]$, it is reasonable to have some error.

The derivation of the IVT method lacks some clearity. As it is not a direct implementation of the intermediate value theorem, it would be good to add references here and/or explain it more direct. E.g. the six cases in Figure 1 are not clearly written somewhere. It would be helpful to put headlines above the graphs mentioning the order. So for example it is not clear to me, why the Figure did not contain a case that is delta_a1<deltav1<deltav2<delta_a2, because this would also fulfill k1*k2<0.

Response: Thanks for the comment. Appendix of IVT method has been added as follows.

"**Proposition.** In the traditional linear Keeling plot system, denote $\delta_a = f(t)$, $\delta_v = g(t)$, $\delta_{ET} = h(t)$ and $C_a = I(t) > 0$ as a continuous function of time. And for two definite moments t_1 and t_2 ($t_1 < t_2$), $\delta_{a_1} \neq \delta_{a_2} \neq \delta_{v_1} \neq \delta_{v_2} \neq \delta_{ET_1} \neq \delta_{ET_2}$. The slopes of corresponding keeling plot curve are $k_1 = C_{a_1}(\delta_{a_1} - \delta_{ET_1})$ and $k_2 = C_{a_2}(\delta_{a_2} - \delta_{ET_2})$, respectively. Then we have that when $k_1 k_2 < 0$, there exists $[t_1', t_2'] \subset [t_1, t_2]$, such that $[min(f(t_1'), f(t_2')), max(f(t_1'), f(t_2'))] \subset [min(\delta_{v_1}, \delta_{v_2}), max(\delta_{v_1}, \delta_{v_2})]$.

"**Remark**: To make a proof of the proposition, classical Intermediate Value Theorem (IVT) was used. It states that if f is a continuous function from the interval $I = [a, b]$ to real number (R). Then *Version I.* if u is a number between $f(a)$ and $f(b)$, there is *c* in (a, b) such that $f(c) = u$. *Version II*. the image set $f(I)$ is also an interval, and it contains $[min(f(a), f(b)), max(f(a), f(b))]$. While in this study, IVT was able to be explained as follows: if f is a continuous function from the interval $I = [t_1, t_2]$ to R with $min[f(t_1), f(t_2)] < \delta_v$ and $max[f(t_1), f(t_2)] > \delta_v$, then *Version I* implies that there is $t' \in (t_1, t_2)$ such that $f(t') = \delta_v$. And *Version II* implies that the image set $f(I)$ is also an interval, and it contains $[min(f(t_1), f(t_2)), max(f(t_1), f(t_2))]$.

"**Proof.** Since $k_1k_2 < 0$, we have $\delta_{a_1} < \delta_{v_1}$ and $\delta_{a_2} > \delta_{v_2}$, or $\delta_{a_1} > \delta_{v_1}$ and $\delta_{a_2} < \delta_{v_2}$. As a result, the cases $\delta_{a_1} < \delta_{v_1} < \delta_{a_2} < \delta_{v_2}$, $\delta_{v_1} < \delta_{a_1} < \delta_{v_2} < \delta_{a_2}$, $\delta_{v_2} < \delta_{a_2} < \delta_{v_1} < \delta_{a_1}$, $\delta_{a_2} < \delta_{v_2} < \delta_{a_1} < \delta_{v_1}$ and $[min(\delta_{v_1}, \delta_{v_2}), max(\delta_{v_1}, \delta_{v_2})] \cap [min(\delta_{a_1}, \delta_{a_2}), max(\delta_{a_1}, \delta_{a_2})] = \emptyset$ do not meet the precondition $k_1k_2 < 0$. There are only four cases below. We will prove the proposition in each of the four cases.

Case 1: $[min(\delta_{v_1}, \delta_{v_2}), max(\delta_{v_1}, \delta_{v_2})] \subset [min(\delta_{a_1}, \delta_{a_2}), max(\delta_{a_1}, \delta_{a_2})]$ (**Fig. 1 a**).

According to IVT *Version I*, there exists $t_1' \in [t_1, t_2]$, such that $f(t_1') = \delta_{v_1}$; similarly, there exists $t_2' \in [t_1, t_2]$, such that $f(t_2') = \delta_{v_2}$. Based on IVT *Version II*, there exists $[t_1', t_2'] \subset [t_1, t_2]$, such that $[min(f(t_1'), f(t_2')), max(f(t_1'), f(t_2'))] = [min(\delta_{v_1}, \delta_{v_2}), max(\delta_{v_1}, \delta_{v_2})]$.

Case 2: $[min(\delta_{a_1}, \delta_{a_2}), max(\delta_{a_1}, \delta_{a_2})] \subset [min(\delta_{v_1}, \delta_{v_2}), max(\delta_{v_1}, \delta_{v_2})]$ (**Fig. 1 b**).

According to IVT *Version I*, there exists $t_1' \in [t_1, t_2]$, such that $f(t_1') = \delta_{a_1}$; similarly, there exists $t_2' \in [t_1, t_2]$, such that $f(t_2') = \delta_{a_2}$. Based on IVT *Version II*, there exists $[t_1', t_2'] \subset [t_1, t_2]$, such that $[min(f(t_1'), f(t_2')), max(f(t_1'), f(t_2'))] = [min(\delta_{a_1}, \delta_{a_2}), max(\delta_{a_1}, \delta_{a_2})] \subset [min(\delta_{v_1}, \delta_{v_2}), max(\delta_{v_1}, \delta_{v_2})]$.

Case 3: $\delta_{v_2} < \delta_{a_1} < \delta_{v_1} < \delta_{a_2}$, or $\delta_{a_2} < \delta_{v_1} < \delta_{a_1} < \delta_{v_2}$ (**Fig. 1 c** and **Fig. 1 d**).

According to IVT *Version I*, there exists $t_2' \in [t_1, t_2]$, such that $f(t_2') = \delta_{v_1}$. Given case (2), when $[\min(\delta_{a_1}, \delta_{v_1}), \max(\delta_{a_1}, \delta_{v_1})] \subset [min(\delta_{v_1}, \delta_{v_2}), max(\delta_{v_1}, \delta_{v_2})]$, there exists $[t_1', t_2'] \subset [t_1, t_2'] \subset [t_1, t_2]$, such that $[min(f(t_1'), f(t_2')), max(f(t_1'), f(t_2'))] \subset [min(\delta_{a_1}, \delta_{v_1}), max(\delta_{a_1}, \delta_{v_1})] \subset [min(\delta_{v_1}, \delta_{v_2}), max(\delta_{v_1}, \delta_{v_2})]$.

Case 4: $\delta_{v_1} < \delta_{a_2} < \delta_{v_2} < \delta_{a_1}$, or $\delta_{a_1} < \delta_{v_2} < \delta_{a_2} < \delta_{v_1}$ (**Fig. 1 e** and **Fig.1 f**).

According to IVT *Version I*, there exists $t_1' \in [t_1, t_2]$, such that $f(t_1') = \delta_{v_2}$. Based on case (2), when $[\min(\delta_{a_2}, \delta_{v_2}), \max(\delta_{a_2}, \delta_{v_2})] \subset [min(\delta_{v_1}, \delta_{v_2}), max(\delta_{v_1}, \delta_{v_2})]$, there exists $[t_1', t_2'] \subset [t_1', t_2] \subset [t_1, t_2]$, such that $[min(f(t_1'), f(t_2')), max(f(t_1'), f(t_2'))] \subset [min(\delta_{a_2}, \delta_{v_2}), max(\delta_{a_2}, \delta_{v_2})] \subset [min(\delta_{v_1}, \delta_{v_2}), max(\delta_{v_1}, \delta_{v_2})]$.

Thus the proposition is true for all four possible scenarios, which make the estimation of δ_a theoretically feasibly when $k_1k_2 < 0$ and δ_{v_1} and δ_{v_2} adequately close. Actual δ_a between t_1 and t_2 can be ensured in the interval $[min(\delta_{v_1}, \delta_{v_2}), max(\delta_{v_1}, \delta_{v_2})]$. To simplify the result, actual δ_a between t_1 and t_2 can be approximately regarded as what Eq. (7) reveals."

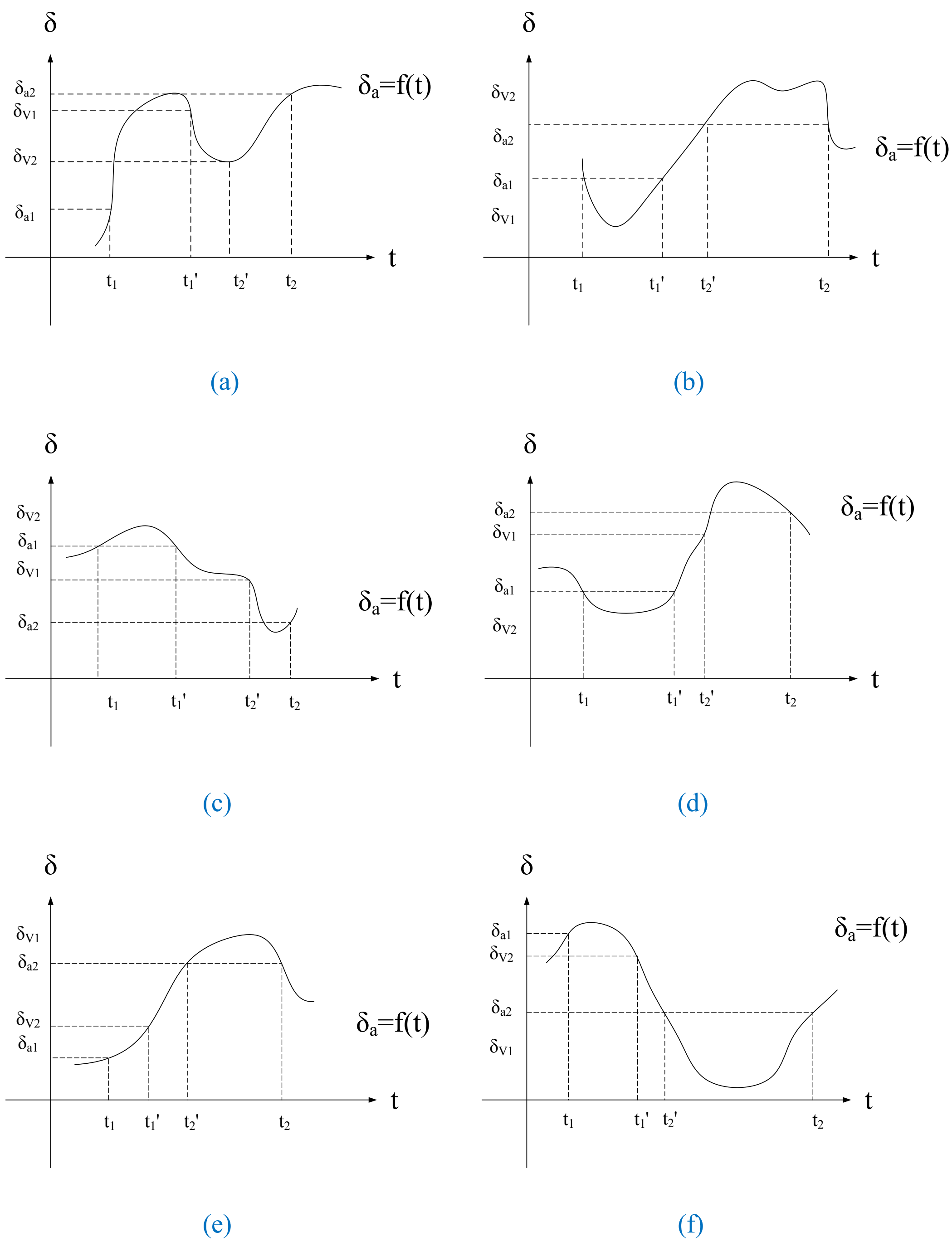

Fig. 1 Theoretical diagrams of all possible combinations of the relationships between isotope composition of ambient vapor (δ_a) and observed isotope composition of atmospheric vapor (δ_v) of two continuous moments t_1 and t_2, ($t_1 < t_2$). δ_{a1} and δ_{a2} represent δ_a value in t_1 and t_2, respectively. δ_{v1} and δ_{v2} represent δ_v value in t_1 and t_2, respectively. t_1' and t_2' represent the time of two specific moments between t_1 and t_2 with $t_1 < t_1' < t_2' < t_2$. For all of the six situations, there exists some sub-intervals $[t_1', t_2'] \subset [t_1, t_2]$ such that the whole range of $\{\delta_a(t): t \in [t_1', t_2']\}$ is within $[min(\delta_{v_1}, \delta_{v_2}), max(\delta_{v_1}, \delta_{v_2})]$.

I would recommend a detailed language check and in general a more careful usage of definitions, because there are some language-related unclearities that might be avoided by a more precise description.

Response: We performed a detailed language check throughout the manuscript, as suggested.

Some minor comments:

It is not clearly written how Eq. 6 is used. I guess delta_ET is taken from two adjacent Keeling plots, but which c_v and delta_v are taken. One more sentence would help here.

Response: Apologize. Eq. 6 is a mistake. Revision has been made.

The calibration procedure is not explained. E.g. it is not clear to me, what is meant in line 173. If this refers to a standard procedure, a reference would help.

Response: Explained above.

Line 270: I am not sure if the IVT method really gives an explanation for the figure as stated here, or if it is rather the other way around, that the figure can be used to understand the IVT method and in particular the change of slope.

Response: Explained above.

I think the reference to equation 1 in line 197 is wrong.

Response: Sorry we do not find any equations in line 197. Equation 1 is in line 93. It is a commonly used water balance equation.

Novel Keeling plot based methods to estimate the isotopic composition of ambient water vapor

Style Definition: Heading 1

Yusen Yuan[a,b], Taisheng Du[a]*, Honglang Wang[c], Lixin Wang[b]*

[a] Center for Agricultural Water Research in China, China Agricultural University, Beijing 100083, China

[b] Department of Earth Sciences, Indiana University-Purdue University Indianapolis, Indianapolis, Indiana 46202, USA

[c] Department of Mathematical Sciences, Indiana University-Purdue University Indianapolis, Indianapolis, Indiana 46202, USA

* Corresponding author: Dr. Taisheng Du
Fax: +86-10-62737611; Tel: +86-10-62738398
Email: dutaisheng@cau.edu.cn

* Corresponding author: Dr. Lixin Wang
Fax: +1-1-317-274-7966; Tel: +1-317-274-7764
Email: lxwang@iupui.edu

Highlights:

1. Two new methods were developed to estimate the isotopic composition of ambient vapor.
2. Theoretical derivations were provided for these two methods.
3. Linear regression showed strong agreement between the two methods.
4. The methods provide a possibility to calculate the proportion of evapotranspiration fluxes to total atmospheric vapor using the same instrumental setup for the traditional Keeling plot investigations.

Abstract

Keeling plot approach, a general method to identify the isotopic composition of source atmospheric CO_2 and water vapor (i.e., evapotranspiration), has been widely used in terrestrial ecosystems. The isotopic composition of ambient water vapor (δ_a), an important source of atmospheric water vapor, is not able to be estimated to date using the Keeling plot approach. Here we proposed two new methods to estimate δ_a using the Keeling plots: one using intersection point method and another relying on the Intermediate Value Theorem. As actual δ_a value was difficult to measure directly, we used two indirect approaches to validate our new methods. First, we made an external vapor tracking using Hybrid Single Particle Lagrangian Integrated Trajectory (HYSPLIT) model to facilitate explaining the variation of δ_a. The trajectory vapor origin results were consistent with the expectations of the δ_a values estimated by these two methods. Second, regression analysis was used to evaluate the relationship between δ_a values estimated from these two independent methods and they are in strong agreement. This study provides an analytical framework to estimate δ_a using existing facilities, and provides important insights into the traditional Keeling plot approach by showing: a) a possibility to calculate the proportion of evapotranspiration fluxes to total atmospheric vapor using the same instrumental setup for the traditional Keeling plot investigations, and b) perspectives on estimation of isotope composition of ambient CO_2 ($\delta_a{}^{13}C$).

Key words: HYSPLIT, intersection point, Intermediate Value Theorem, Keeling plot, stable isotope

Deleted: other

Deleted: curve

Deleted: p

Deleted: intermediate

Deleted: value

Deleted: theorem

Deleted: (a) an evidence that δ_a was constant in a certain moment among different heights, a key assumption of the Keeling plot approach, (b

Deleted: c

1. Introduction

Stable isotopes of hydrogen and oxygen ($^{1}H^{2}HO$ and $H_2^{18}O$) have been widely used in root water uptake source identification (Corneo et al., 2018, Mahindawansha et al., 2018, Lanning et al., 2020) and evapotranspiration (ET) partitioning (Brunel et al., 1997; Wang et al., 2010; Cui et al., 2020) in terrestrial ecosystems based on Craig-Gordon model (Craig and Gordon, 1965), isotope mass balance and mechanisms of isotopic fractionation (Majoube, 1971; Merlivat and Jouzel, 1979). With the advent of laser isotope spectrometry capable of high frequency (1 Hz) measurements of the isotopic composition of atmospheric water vapor (δ_v) and atmospheric water vapor content (C_v) (Kerstel and Gianfrani, 2008; Wang et al., 2009), the number of studies based on high frequency ground-level isotope measurements was continuously increasing. These studies generate new insights into the processes that affect δ_v, including meteorological factors (Galewsky et al., 2011; Steen-Larsen et al., 2013), biotic factors (Wang et al., 2010) and multiple factors (Parkes et al., 2016). Such increase in δ_v measurements allows an isotope-enabled global circulation models (Iso-GCMs) to estimate the variation of water vapor isotope parameters at a global scale (Werner et al., 2011). Concomitantly, more than δ_v, several new methods using high frequency ground-level isotope measurements were devised to directly estimate the isotopic composition of leaf water (Song et al., 2015) and leaf transpired vapor (Wang et al., 2012).

Evapotranspiration is a crucial component of water budget across scales such as field (Wagle et al., 2020), watershed (Zhang et al., 2001), regional (Hobbins et al., 2001) and global (Jung et al., 2010) scales. The water isotopic composition of ET (δ_{ET}) was generally estimated by Keeling plot approach (Keeling, 1958). It was first used to explain carbon isotope ratios of

Formatted: No bullets or numbering

Deleted: ; Mahindawansha et al., 2018… and evapotranspiration (ET) partitioning (Brunel et al., 1997; Wang et al., 2010; Cui et al., 2020) in terrestrial ecosystems based on Craig-Gordon model (Craig and Gordon, 1965), isotope mass balance and mechanisms of isotopic fractionation (Majoube, 1971; Merlivat and Jouzel, 1979). With the advent of laser isotope spectrometry capable of After laser spectrometers being utilized to perform ... [1]

Deleted: continuous …igh frequency (1 Hz) measurements of the isotopic composition of atmospheric water vapor (δ_v) and atmospheric water vapor content (C_v) (Kerstel and Gianfrani, 2008; Wang et al., 2009), the number of studies based on high frequency continuous …round- …evel isotope measurements was continuously increasing,… These studies generating … new insights into the processes that affect δ_v, including meteorology ... [2]

Deleted: new insights into processes that affect δ_v and the ... [3]

Formatted: Font color: Auto

Deleted: For example, …uch increase in δ_v isotope data ... [4]

Deleted: abundanc…easurementse ... [5]

Deleted: an…an isotope-enabled global circulation models ... [6]

Formatted: Font color: Blue

Deleted: (Unger et al., 2010)

Moved down [2]: Concomitantly, several gas exchange

Deleted:

Moved (insertion) [2]

Deleted: gas exchange chamber-based

Formatted ... [7]

Deleted: These studies provide a guidance that the ... [8]

Formatted: Font color: Auto

Deleted: among

Formatted ... [9]

Deleted: ,

Formatted: Font color: Auto

Deleted: watershed (Zhang et al., 2001)

Formatted ... [10]

Deleted: generally

Deleted: often…enerally estimated by Keeling plot approach ... [11]

atmosphere CO_2 and to identify the sources that contribute to increases in atmospheric CO_2 concentration, and has been further used to estimate δ_{ET} in recent two decades (Yakir and Sternberg, 2000). Keeling plot analyses can be applied using δ_v and C_v output by laser based analyzer either from different heights (Yepez et al., 2003; Zhang et al., 2011; Good et al., 2012) or at one height with continuous observations (Wei et al., 2015; Keppler et al., 2016). Although the intercept of the linear regression line was commonly used as estimated δ_{ET}, the slope of the Keeling plot was also used to estimate δ_{ET} by re-arranging the Keeling plot equations (Miller and Tans, 2003; Fiorella et al., 2018). Keeling plot approach was based on isotope mass balance and two-source assumption using two equations with three unknowns. As a result, the isotopic composition of other potential sources (e.g., water vapor not from ET), as well as isotopic composition of ambient water vapor (δ_a), were not able to be estimated directly using the Keeling plot approach. That is one of the reasons why field scale moisture recycling is difficult to estimate to date.

In this study, we proposed two new methods to estimate δ_a, one based on the intersection of two Keeling plots of two continuous observation moments and the other based on the Intermediate Value Theorem. Proposition and proof were provided, and the new methods were tested using field observations. As direct observations of δ_a rarely exist (Griffis et al., 2016), we tested our methods by (a) making an external water vapor tracking investigation according to HYSPLIT model to explain the variation of estimated δ_a, and (b) making a regression analysis on daily scale and point to point scale using δ_a estimated by these two independent methods.

Deleted: . It

Deleted: isotopic composition of ET (

Deleted:)

Deleted: da SL

Deleted: curve

Deleted: was based on bulk water and isotope mass balance

Deleted: should be as essential as δ_{ET},

Deleted: another

Deleted: intermediate

Deleted: value

Deleted: theorem

2. Materials and Methods

2.1 Theory

The atmospheric vapor concentration in an ecosystem reflects the combination of ambient vapor that is already exist in the atmosphere and the vapor that is added through evaporation (E) and transpiration (T) (Yakir and Sternberg, 2000). Keeling plot approach is based on the combination of a bulk water mass balance equation and an isotope mass balance equation:

$$C_v = C_a + C_{ET} \quad , \quad (1)$$

$$C_v \delta_v = C_a \delta_a + C_{ET} \delta_{ET} \quad , \quad (2)$$

where δ_a, δ_{ET} and δ_v are isotope composition of ambient water vapor, ET, and atmospheric water vapor, respectively, and C_a, C_{ET} and C_v are the corresponding concentrations of water vapor. Note that all quantities here are time dependent, and δ_v and C_v also depend on heights.

Combining Eq. (1) and Eq. (2), we have the following traditional linear Keeling plot relationship between δ_v and $1/C_v$ with intercept δ_{ET} and slope $C_a(\delta_a - \delta_{ET})$,

$$\delta_v = C_a(\delta_a - \delta_{ET})/C_v + \delta_{ET} \quad . \quad (3)$$

For a given time, with various measurements of δ_v and C_v collected at different heights, we are able to estimate the intercept δ_{ET} and slope $k = C_a(\delta_a - \delta_{ET})$ for this moment from regression analysis (Zhang et al., 2011; Wang et al., 2013). Here we focus on the estimation of δ_a using two new methods proposed below.

Intersection point (IP) method. Note that for two nearby time points t_1 and t_2, we could use local constant approximation to estimate δ_a within this time interval since it remains relatively constant over a short period of time. By assuming local constant for C_a and δ_a within

Formatted: No bullets or numbering

Deleted: da SL

Deleted: it is changing smoothly over time this time interval, we have

$$k_1 = C_a(\delta_a - \delta_{ET_1}) \quad , \qquad (4)$$

$$k_2 = C_a(\delta_a - \delta_{ET_2}) \quad , \qquad (5)$$

where k_i and δ_{ET_i} represent the value at t_i for i=1, 2. From (4) and (5), we can solve δ_a as:

$$\delta_a = \frac{k_1\delta_{ET_2} - k_2\delta_{ET_1}}{k_1 - k_2} \quad . \qquad (6)$$

The local constant approximation idea was first described in Yamanaka and Shimizu (2007) as an assumption to quantify the contribution of local ET to total atmospheric vapor.

Intermediate Value Theorem (IVT) method. Denote the slope as $k = C_a(\delta_a - \delta_{ET})$. Since $C_a < C_v = C_a + C_{ET}$, we have $C_a = \frac{k}{(\delta_a - \delta_{ET})} < C_v$. We can rearrange $\frac{k}{(\delta_a - \delta_{ET})} < C_v$ to attain δ_a: $\delta_a < \frac{k}{C_v} + \delta_{ET} = \delta_v$ when $k < 0$, and $\delta_a > \frac{k}{C_v} + \delta_{ET} = \delta_v$ when $k > 0$.

For the smooth function $\delta_a(t)$ defined on the interval $[t_1, t_2]$ with the two time points satisfying $k(t_1)\,k(t_2) < 0$, depending on the sign of the slopes $k(t_1)$ and $k(t_2)$ and the order of $\delta_{v_1} = \delta_v(t_1)$ and $\delta_{v_2} = \delta_v(t_2)$ at the two time points t_1 and t_2, it will correspond to one of the situations in **Fig. 1**. For all of the situations, by the Intermediate Value Theorem, there exists a sub-interval $[t_1', t_2'] \subset [t_1, t_2]$ such that the whole range of $\{\delta_a(t): t \in [t_1', t_2']\}$ is within $[min(\delta_{v_1}, \delta_{v_2}), max(\delta_{v_1}, \delta_{v_2})]$. Proof details of this proposition is shown in the appendix. Thus for the two nearby time points t_1 and t_2 with k_1 and k_2 having different signs, δ_a will be between δ_{v_1} and δ_{v_2}. This provides a prerequisite for estimating the parameter of interest δ_a based on Intermediate Value Theorem, which leads to approximation of δ_a within the time interval between t_1 and t_2 using δ_{v_1} and δ_{v_2}:

$$\delta_a \approx \frac{\delta_{v_1} + \delta_{v_2}}{2} \quad . \qquad (7)$$

Using this method, we are able to compute δ_a using data points when the slopes of

Deleted:

Deleted: , δ_{v_i} and C_{v_i}

Deleted: intermediate

Deleted: value

Deleted: theorem

Deleted: on

Deleted: part

Deleted: is

Deleted: the key observation to estimate

Keeling plots change signs between two adjacent time points.

2.2 Field observations

2.2.1 Study site

A field measurement was conducted over a maize field (39 ha) from 1st May 2017 to 30st September 2017 at Shiyanghe Experimental Station of China Agricultural University, located in Wuwei of Gansu Province, northwest China (37°85′N, 102°88′E; altitude 1581m). The region belongs to temperate continental climate and is in the oasis within the Shiyang river basin. The annual mean temperature of the study area is about 8.8℃ with pan evaporation of 2000 mm, annual precipitation of 164.4 mm, mean sunshine duration of 3000 h, and frost-free period of more than 150 d. The local crops are irrigated using groundwater with electrical conductivity of 0.62 dSm^{-1}. The groundwater table is 30-40 m below the surface. Maize was sowed on April and harvested on September 2017, with row spacing of 40 cm and plant spacing of 23 cm. The maize growing stage was divided into seedling stage (April 21st –May 20th), jointing stage (May 21st-July 10th), heading period (July 11th-July 31st), pustulation period (August 1st-August 31st) and mature period (September 1st-September 20th).

Deleted: 1st

Deleted: 23

Deleted: 15

2.2.2 Instrument setup and measurement design

A 24-meter flux tower, located in the middle of maize field, was used to measure ET flux and isotopic composition of water vapor at different heights. The field is approximately 600 m long and 240 m wide, with a 10% slope decreasing from southwest to northeast. Five gas traps were installed on the flux tower at heights of 4 m, 8 m, 12 m, 16 m and 20 m, respectively. An iron pillar was placed 20 m away from the flux tower. Three gas traps were installed on the iron pillar, one was close to the canopy, and the other two were 2 m and 3 m above the ground.

Canopy gas trap was adjusted weekly according to the height of maize.

In situ δ_v and C_v collected by the eight gas traps were monitored by a water vapor isotope analyzer (L2130-i, Picarro Inc., Sunnyvale, CA, USA), which was a wavelength scanned cavity ring down spectroscope (WS-CRDS) instrument. Vapor specifications include a measurement range from 1000 to 50000 ppm, the precision is 0.040‰ to 0.25‰ for $\delta^{18}O$ (Zhao et al., 2019). Interfacing with the gas trap and the isotope analyzer, teflon tube was wrapped by thermal insulation cotton to avoid vapor condensation during transmission. The measurement of δ_v and C_v were conducted from May to September, which should have 153 days of data. Forty-nine days among them were complete with 24-hour continuous datasets. There were missing data for either a whole day or several hours of a day for other days due to the maintenance of the analyzer. These 49 days was chosen in our study for data analysis.

2.2.3 Calibration of δ_v and C_v

Our calibration procedure mainly followed the study by Steen-Larsen et al. (2013) with some modifications to fit our specific experimental setup. The water vapor from eight inlets were sampled continuously over a 24-hour-period. Since only one analyzer was used to measure the δ_v and C_v, the values of eight sampling inlets were recorded in turn every 225s in a 30 mins cycle. The switch procedure was automatic. As the analyzer makes a measurement every 0.9-1s, approximately 259-264 values for each inlet was recorded within the cycle. For each 225s measurement period, No. 195 to No. 253 data points were used to avoid memory issue and influence of transient pressure variation. The absolute value of coefficient of variations (|CV|) of δ_v and C_v were no more than 0.016 and 0.002, respectively, which was far below the critical value of 15% (Lovie, 2005). The mean value of the selected data points was regarded as the

Deleted: n

Deleted: isotope and gas concentration analyzer

Deleted: Teflon

Deleted: on

Deleted: on

Deleted: for 19th May, 11th June, 20th July, and 12th August

Deleted: 49

Deleted: and

Deleted: continuous

Deleted: While other days were lack of data

Deleted: of data

Deleted: were selected to test the theoretical framework because they fit the criteria requirements of the IP method and IVT method: 1) a complete and continuous 24-hour dataset and 2) opposite Keeling plots slope occurrence at least once in a day. These four days corresponded to seedling stage, jointing stage, heading stage, and pustulation stage, respectively, through the maize growth period.

Formatted: Font color: Auto

Deleted: referred to

Formatted: Font color: Auto

Deleted: . Moreover, we had some different measures to fit our study, which were carefully evaluated

Formatted: Font color: Auto

Formatted: Font color: Auto

Formatted: Font color: Auto

measured δ_v and C_v in a specific inlet. Measured C_v was used directly as actual C_v, while measured δ_v was calibrated to minimize the influence of isotopic concentration dependence. The C_v in our measurement ranged from 5386 ppm to 30255 ppm. Thus, C_v gradients of 10000 ppm, 20000 ppm and 30000 ppm were selected as calibration concentrations to improve the precision of δ_v.

2.3 Data quality control for δ_a estimation

With a 30-min interval for 49 days, we should in theory produce 2352 δ_a values for both IP method and IVT method. However, because of the precondition of $k_1k_2<0$ required for the IVT method, 166 δ_a values was able to be calculated using the IVT method ($\delta_{a(IVT)}$). δ_a values using the IP method ($\delta_{a(IP)}$) was not restricted by this precondition. Furthermore, a filter ($\delta_{ET}<\delta_v<\delta_a$ or $\delta_{ET}>\delta_v>\delta_a$) was used for both methods because δ_v was a mixture of δ_{ET} and δ_a. Therefore, δ_a values that meet both precondition $k_1k_2<0$ and the condition of $\delta_{ET}<\delta_v<\delta_a$ or $\delta_{ET}>\delta_v>\delta_a$ were considered satisfying the criteria for the IVT method; δ_a values that meet the condition of $\delta_{ET}<\delta_v<\delta_a$ or $\delta_{ET}>\delta_v>\delta_a$ were considered satisfying the criteria for the IP method. In the end, we obtained 1264 and 103 δ_a values using IP and IVT methods, respectively (**Table 1**). Eighty eight time points were overlapped between the $\delta_{a(IP)}$ and $\delta_{a(IVT)}$ based δ_a results. These 88 time points were selected to test the reliability of two methods at point to point scale. During the 49 days, there were 21 days when more than one $\delta_{a(IVT)}$ was attained for each day. These 21 days was also used to investigate the time series of daily scale δ_a variations and other isotopic variations. Further analysis in section 2.4 in the following was made on these 21 days.

2.4 Explanations of δ_a using backward trajectories

To explain the variations of estimated δ_a, air mass backward trajectories were calculated

Deleted: Counting process and filter basis

Formatted: Indent: First line: 0.4", No bullets or numbering

Deleted: in…or 49 days, we should in theory have gotten…roduce 2352 δ_a values with…or both IP method and IVT method, respectively… However, as…ecause of the precondition of $k_1k_2<0$ required for the IVT method, 166 of 2352 …$_a$ values using IVT method ($\delta_{a(IVT)}$) …as able to be calculated using the IVT method ($\delta_{a(IVT)}$). δ_a values using the IP method ($\delta_{a(IP)}$) was not restricted by this precondition. Furthermore, a filter ($\delta_{ET}<\delta_v<\delta_a$ or $\delta_{ET}>\delta_v>\delta_a$) was made…sed for both methods to express the relationship that…ecause δ_v was the… mixture of δ_{ET} and δ_a. Therefore, We defined the …$_a$ values after …hat meet the ... [12]

Formatted: Not Highlight

Deleted: filter

Formatted: Not Highlight

Deleted: (

Formatted: Not Highlight

Deleted:)

Formatted ... [13]

Deleted:

Formatted ... [14]

Deleted: as the δ_a values meet the criteria… Finally…n the end, we obtained 1264 $\delta_{a(IP)}$ …nd 103 δ_a values meet the criteria …sing IP and IVT methods$\delta_{a(IVT)}$… respectively (**Table.…1**). 88…ighty eight time points thereinto …ere overlapped to acquire both…etween the $\delta_{a(IP)}$ and $\delta_{a(IVT)}$ based δ_a results. These 88 time points were selected to test the reliability of two methods in ... [15]

Formatted: Subscript

Deleted: Moreover, w

Deleted: Thesewas used thetime series of -variations other s

Deleted: In these 21 days, we were able to obtain more than one $\delta_{a(IVT)}$ in each day.

Deleted: 3

Formatted: Normal, No bullets or numbering using the Hybrid Single Particle Lagrangian Integrated Trajectory (HYSPLIT) model (Draxler and Hess, 1997; Draxler, 2003; Stein et al., 2015; Kaseke et al., 2018) and meteorological data from the Global Data Assimilation System 0.5 Degree (GDAS0p5) with 0.5°×0.5° spatial resolution and 3-hour time resolution for the 21 days mentioned in section 2.3. Five hundred meters height was selected in the modeling. Each backward trajectory was initialized from the station (37°85′N, 102°88′E) at 12:00 pm (local time), and calculated backward for 72 hours. Eighteen trajectories were computed, except for June 21st, August 18th and September 29th when vertical velocity data were missing. Finally, we used these 18 trajectories represented the vapor origin in the corresponding 18 days.

3. Results

3.1 Time series variations of δ_{ET}, δ_v, δ_a and k

Time series of isotopic variations were shown in **Fig. 2**. The δ_v here is the average value of eight heights. The average δ_{ET}, δ_v, $\delta_{a(IP)}$ and $\delta_{a(IVT)}$ were -11.04‰, -13.00‰, -13.60‰ and -13.29‰, respectively in those 21 days when more than one $\delta_{a(IVT)}$ was attained for each day. Daytime (7:00am-7:00pm) average δ_{ET}, δ_v, $\delta_{a(IP)}$ and $\delta_{a(IVT)}$ were -10.73‰, -13.33‰, -14.08‰ and -13.63‰, respectively. While at nighttime (7:00pm-7:00am the next day), average δ_{ET} was lower than that at daytime, which was on the contrary with δ_v, $\delta_{a(IP)}$ and $\delta_{a(IVT)}$. The trend of $\delta_{a(IP)}$ and $\delta_{a(IVT)}$ were similar to δ_v. In majority of circumstances, δ_{ET} is the largest of those four isotopic parameters, except on May 19th, June 4th and June 9th. About 76% of k values were negative, and most positive k values occurred at nighttime (60%). The percentage of positive k values were 33%, 34%, 24%, 34% and 10% in May, June, July, August and September, respectively. Standard deviation were used here to evaluate the constancy among isotopic parameters at daily scale. The standard deviation of δ_{ET}, δ_v, $\delta_{a(IP)}$ and $\delta_{a(IVT)}$ were 6.08‰, 0.91‰, 1.38‰ and 0.59‰, respectively. Therefore, the constancy of δ_a was similar to the constancy of δ_v at daily scale.

3.2 Daily variations of HYSPLIT backward trajectories and δ_a using two methods

The 500 m height water vapor backward trajectories revealed that water vapor was from outside the study regions for ten days (**Fig. 3a**), and water vapor was from local ET for eight days (**Fig. 3b**).

As for the IP method, 53.7% of $\delta_{a(IP)}$ values met the criteria, and 49.4% of $\delta_{a(IP)}$ values meeting the criteria were during the daytime (7:00am-7:00pm). The range of $\delta_{a(IP)}$ values meeting the criteria were between -16.79‰ and -12.95‰ for the ten days with external origins (**Fig. 3a**). The range of $\delta_{a(IP)}$ values meeting the criteria were between -12.77‰ and -9.51‰ for the eight days with local origins (**Fig. 3b**).

As for the IVT method, only 4.4% of δ_a values met the criteria, and 35.9% of δ_a values meeting the criteria were during the daytime (7:00am-7:00pm). The range of $\delta_{a(IVT)}$ values meeting the criteria were between -16.31‰ and -13.93‰ for the ten days with external origins (**Fig. 3a**). The range of $\delta_{a(IVT)}$ values meeting the criteria were between -12.67‰ and -9.12‰ for the eight days with local origins (**Fig. 3b**).

3.3 Linear regression between $\delta_{a(IP)}$ and $\delta_{a(IVT)}$

Method comparison was made at both daily scale (**Fig. 4a**) and point to point scale (**Fig. 4b**). The 21 days (see method section 2.3) in **Fig. 3a** and **Fig. 3b** were selected to figure out the daily scale relationship between $\delta_{a(IP)}$ and $\delta_{a(IVT)}$. Point to point scale data was based on the 88 point of overlapped $\delta_{a(IP)}$ and $\delta_{a(IVT)}$ (see method section 2.3) among all 49 days, which

Deleted: Std(
Formatted: Font color: Auto
Deleted:)… Std(…v)… Std(…a(IP))…and Std(…a(IVT)) ... [26]
Formatted ... [27]
Deleted: As a result
Formatted: Font color: Auto
Moved down [1]: The 500 m height water vapor backward
Deleted: Diurnal
Formatted: Font: (Default) +Body (Times New Roman)
Deleted: during the maize growing period
Moved (insertion) [1]
Deleted: on…or ten days in ... [28]
Formatted: Font: Bold
Deleted: (
Deleted:
Deleted: .
Deleted: 19th May and 20th July…w ... [29]
Deleted: While…nd water vapor was from local ET on ... [30]
Deleted: 11th June and 12th August
Deleted: in
Formatted: Font: Not Bold
Deleted: (
Deleted: (
Deleted: Data screening was needed on the calculation of δ_a ... [31]
Formatted: Indent: First line: 0.4"
Deleted: 46.8…3.7% of $\delta_{a(IP)}$ values met the criteriawere ... [32]
Deleted: (
Deleted: -…16.7912.95 ... [33]
Deleted: ,
Deleted: -12.13
Deleted:)…on…or the tenn…days with external origins ... [34]
Deleted: ,
Deleted: While t…he range of $\delta_{a(IP)}$ values meeting the ... [35]
Deleted:
Deleted:)…on…or the eight days in…ith local origins (Fig. ... [36]
Deleted: -14.39‰ and -12.77‰ for the four days, ... [37]
Deleted: 13.8….4% of δ_a values met the criteriawere ... [38]
Deleted: (…etween -16.31‰,…and -13.93‰ for the ten ... [39]
Deleted: The average δa values were -13.93‰, -11.03‰, ... [40]
Formatted ... [41]
Formatted ... [42]
Formatted: Heading 2
Deleted: both on
Formatted ... [43]
Deleted: Fourteen observation periods …verlapped $\delta_{a(IP)}$ and ... [44]

accounted for 7.0% of δ_a values using IP method and 85.4% of δ_a values using IVT method. Linear regression between $\delta_{a(IP)}$ and $\delta_{a(IVT)}$ was significant at both daily scale and point to point scale. The degree of agreement was less for the daily time scale than point to point scale and the RMES between these two methods at daily scale and point to point scale were 0.618‰ and 0.167‰, respectively.

4. Discussion

4.1 The reliability of δ_a estimating methods

The IP method was based on the assumption that the ambient sources were the same between two continuous observation moments. This is a reasonable assumption for short time intervals. For the IVT method, δ_a was derived from δ_v in two continuous moments when their Keeling plot slopes were opposite. The opposite slopes of the Keeling plots were the only requirement. As δ_v was almost constant in two continuously moments, $\delta_{a(IVT)}$ was able to be constrained into a small range. The derivation was supported by the Intermediate Value Theorem. Therefore, both methods of estimating δ_a were theoretically sound.

The δ_a results were also examined by HYSPLIT backward trajectories to identify the different sources of water vapor, which assesses the reliability of both methods indirectly. Based on the trajectory analysis, water vapor in the study area came from westerlies, northern polar region and local recirculation. Water vapor from southwest monsoon and northwest Pacific were not detected in this study. Based on the isotope variation of meteoric water (Fricke et al., 1999), water vapor from westerlies and northern polar was more ^{18}O depleted than local recycled moisture through ET. It was also reported that the water vapor from outside the study

Deleted: 15.9

Deleted: ($\delta_{a(IP)}$)

Deleted: 53.8

Deleted: ($\delta_{a(IVT)}$)

Deleted: for these fourteen observation periods with slope close to one

Deleted: on

Deleted: on

Formatted: Font color: Auto

Formatted: Font color: Auto

Deleted: (Fig. 4. $\delta_{a(IP)} = 0.95\delta_{a(IVT)} - 0.75$, $R^2 = 0.98$, $p<0.01$, n=14).

Deleted: ¶

Formatted

Formatted: No bullets or numbering

Deleted: i

Deleted: v

Deleted: t

regions will lower δ_v values (Ma et al., 2014; Chen et al., 2015). The calculated δ_a values of the ten days with external sources (**Fig. 3a**) based on the IP method and JVT approach were higher than those of eight days with local origin (**Fig 3b**), which was consistent with our expectation. The results indicate that quantifying δ_a using both the IP method and JVT approach was reliable. The reliability of two methods at point to point scale were also supported by the close relationship of δ_a using these two independent methods. Daily time scale result is less reliable than point to point scale.

4.2 The application of δ_a for moisture recycling

When δ_a was estimated, moisture recycling (e.g., $f_{ET,}$ the contribution of ET fluxes to the total water vapor) can be estimated using the following equations with known δ_a, δ_{ET}, $\delta_{v,}$ C_{ET} and C_v:

$$C_{ET} = C_v \bullet \frac{\delta_a - \delta_v}{\delta_a - \delta_{ET}} \quad , \qquad (8)$$

$$f_{ET} = \frac{C_{ET}}{C_v} \quad , \qquad (9)$$

According to Eq. (8) and Eq. (9), f_{ET} was only related to $\delta_{a,}$ δ_v, and δ_{ET}. These three parameters were obtained for relatively small temporal and spatial scales in this study, making it possible to estimate f_{ET} at a tower scale. The f_{ET} estimate will provide a baseline value for rainfall recycling ratio calculations. Previous studies quantified the contribution of recycled vapor to annul or monthly precipitation in river basins using two-element mixture model (Kong et al., 2013) and three-element mixture (Peng et al., 2011). At the watershed scale, recycled vapor rate refers to the contributions of moisture from terrestrial ET to annul or monthly precipitation (Trenberth, 1999). It is a key part of local water cycle and the atmospheric water vapor balance (Seneviratne et al., 2006; Aemisegger et al., 2014). In our study, the role of f_{ET}

Deleted: on

Deleted: interval intermediate value theorem

Formatted: Font: Bold

Deleted: 11^{th} June and 12^{th} August

Deleted: two

Formatted: Font: Bold

Deleted: intermediate value theorem

Deleted: The reliability of two methods were also supported by the close relationship of δ_a using these two independent methods.

Formatted: Font color: Auto

Deleted: on

Formatted: Font color: Auto

Deleted: δ_V

to regional vapor is similar to the role of recycled vapor rate to annul or monthly precipitation, but f_{ET} was calculated with fine temporal (e.g., hourly) and spatial (i.e., field scale) scales. At the watershed scale, assumption was made that no isotopic fractionation between transpiration and source water (Flanagan et al., 1991); advected vapor was assumed to be the precipitation vapor of the upwind station (Peng et al., 2011). However, the isotope composition of plant transpired vapor is variable in a day especially under non-steady-state conditions (Farquhar and Cernusak, 2005; Lai et al., 2008; Song et al., 2011). In addition, sometimes it is difficult to select an upwind station without precipitation events. In this study, a field site was selected to calculate the proportion of ET fluxes to total atmospheric vapor and f_{ET} was only related to δ_a, δ_v, and δ_{ET} according to Eq. (8) and Eq. (9). This indicates that f_{ET} calculations is possible for small temporal and spatial scales after estimating δ_a using the methods we proposed.

If we assumed that the parameter δ_v in Eq. (8) is the average δ_v value measured from all the eight heights, f_{ET} in this study was 23.3% and 12.7% in May and September 2017 based on daily $\delta_{a(IP)}$ and daily $\delta_{a(IVT)}$, respectively. It was reported that recycled vapor rate in all Shiyang river basin, oasis region, mountain region and desert region were 23%, 28%, 17% and 15%, respectively (Li, et al., 2016; Zhu, et al., 2019). The f_{ET} based on daily $\delta_{a(IP)}$ in our study was close to these earlier studies. The deviation of f_{ET} based on daily $\delta_{a(IVT)}$ compared with previous studies may be because 64.1% of point to point $\delta_{a(IVT)}$ was observed at nighttime. Normally, ET at nighttime is lower than that of daytime. f_{ET} may be underestimated using daily $\delta_{a(IVT)}$. It could also be inferred that f_{ET} estimation using Eq. (9) may be more reliable using daily $\delta_{a(IP)}$ than daily $\delta_{a(IVT)}$.

Deleted: transpiration

Deleted: δ_V

Deleted: among

Formatted: Subscript

Deleted: measured δ_v

Formatted: Subscript

Deleted: among

Deleted: 2017 to

Formatted: Font color: Auto

Formatted: Subscript

Deleted: ir

Deleted: due t

Deleted: be becasue

Deleted: due to

Deleted: relay on

Deleted: rather

4.3 Implications of δ_a

The signature of δ_E and δ_T was first introduced by a hypothetical graph shown on **Fig. 5a** (Moreira et al., 1997). Line 1 and line 2 was idealized Keeling plot with pure T and pure E, and Line 3 was the Keeling plot with mixed T and E. The IVT method in this study provided a general explanation of this figure. As T is a major component of ET in the daytime in non-arid region (Wang et al., 2014), the slope is generally negative. When E dominates ET in an ecosystem, such as in the nighttime in non-arid region or in arid region, the slope should be positive. Mathematically, negative slope is due to $\delta_{ET} < \delta_a$ and positive slope is due to $\delta_{ET} > \delta_a$. It also reflected that IVT method could only be used in non-arid ecosystems to ensure the appearance of transfer plus or minus in Keeling plots' slope. On the contrary, IP method may not be restricted by the type of ecosystems. Yamanaka and Shimizu (2007) used the assumption that δ_a of an area of 219.9 km^2 was represented by the intersection point of two Keeling plot lines in different sites with synchronous measurements and they used the intersection value as an approximate value of δ_a. This study was conducted in a maize field using 30-min interval measurements. The results verified Yamanaka and Shimizu's (2007) assumption in such spatial and temporal scale, and indicate that accurate $\delta_{a(IP)}$ could be estimated from the intersection of two Keeling plots regardless the slope being positive or negative, while the $\delta_{a(IVT)}$ should be restricted in the area between two dotted lines as shown in **Fig. 5b** (i.e., between the minimum value of δ_v in positive slope and the maximum value of δ_v in negative slope). Although IVT method relies on more stringent precondition for data filtering, this method requires a very simple expression, which only need two parameters to be measured according to Eq. (7).

While this study is about water vapor ^{18}O, the "Keeling plot" was first used by (Keeling,

Deleted: , t

1958, 1961) to interpret carbon isotope ratios of mixed CO_2 and to identify the sources that contribute to increases in atmospheric CO_2 concentrations on a regional basis. Compared with ET in water vapor which consists of E and T, net ecosystem CO_2 exchange is comprised of soil respiration (R) and gross primary productivity (GPP). As $^{13}CO_2$ isotopic Keeling plot reveals a positive slope during both daytime and nighttime (Yakir and Wang, 1996; Unger et al., 2010), the IVT method may not be able to estimate ambient $^{13}CO_2$ isotopic composition ($\delta_a{}^{13}C$) since there are no opposite slopes in a day. In such case, the IP method may be implemented in two continuous moments to estimate $\delta_a{}^{13}C$ and may consequently further calculate the contribution of NEE to atmospheric CO_2.

5. Conclusions

In this study, we established two methods to quantify δ_a using intersection point method and the Intermediate Value Theorem method. The IVT method was used under the condition of opposite slope of Keeling plots in two continuously moments. The results of estimated $\delta_{a(IP)}$ and $\delta_{a(IVT)}$ were consistent with the expectation whether it was local origin or external origin using external vapor tracking investigation by HYSPLIT model. The linear regression between $\delta_{a(IP)}$ and $\delta_{a(IVT)}$ was highly significant both on daily time scale and point to point scale.

This study provided insights into the underexplored traditional Keeling plots and provided two methods to estimate δ_a using the same instrumental setup for the traditional Keeling plot investigations. The estimated δ_a will make it possible to calculate the ET contribution to regional vapor at a 30 min interval at field scale. The results indicate that using similar framework, $\delta_a{}^{13}C$ may also solvable by the IP method.

Deleted: is

Deleted: ed

Deleted: (Wagle et al.)

Formatted: Font color: Accent 5

Formatted: No bullets or numbering

Deleted: regional

Deleted: (R^2=0.98, $p < 0.01$)

Deleted: The results shown an evidence that δ_a was constant in a certain moment among different heights, a key assumption of Keeling plot approach.

Deleted: is

6. Acknowledgements

We acknowledge support from the National Natural Science Foundation of China (51725904, 51621061, 51861125103), the National Key Research Program (2016YFC0400207), the Discipline Innovative Engineering Plan (111 Program, B14002), and the President’s International Research Awards from Indiana University and the Division of Earth Sciences of National Science Foundation (EAR-1554894). We thank Dr. Qianning Liu from Jiangxi University of Finance and Economics and Dr. Zhengxiang Chen from Capital Normal University for checking the validity of the Intermediate Value Theorem method.

7. Code and Data availability

Code and data are available on request.

8. Author contribution

YY, TD and LW conceptualized the main research questions. YY collected data and performed the data analyses. YY and LW wrote the first draft. HW contributed to additional data analyses. All the authors contributed ideas and edited the manuscript.

9. Competing interests

There authors declare no competing interests.

10. References

Aemisegger, F., Pfahl, S., Sodemann, H., Lehner, I., Seneviratne, S. I., and Wernli, H.: Deuterium excess as a proxy for continental moisture recycling and plant transpiration, **Atmospheric Chemistry and Physics**, 14, 4029–4054, doi: 10.5194/acp-144029-2014, 2014.

Brunel, J. P., Walker, G. R., Dighton, J. C., and Monteny, B.: Use of stable isotopes of water to determine the origin of water used by the vegetation and to partition evapotranspiration. A case study from HAPEX-Sahel, **Journal of Hydrology**, 188–189, 466–481, doi:10.1016/s0022-1694(96)03188-5, 1997.

Chen, F. L., Zhang, M. J., Ma, Q., Wang, S. J., Li, X. F., and Zhu, X. F.: Stable isotopic

Formatted: No bullets or numbering

Formatted: Heading 1, No bullets or numbering

Formatted: Font: (Default) Times New Roman, (Asian) DengXian

Formatted: Normal, Indent: Left: 0"

Formatted: Heading 1, No bullets or numbering

Formatted: Indent: Left: 0", First line: 0.4"

Formatted: Heading 1, No bullets or numbering

Formatted: Font: (Default) Times New Roman, (Asian) DengXian

Formatted: Normal, Indent: Left: 0"

Deleted:

characteristics of precipitation in Lanzhou city and its surrounding areas, Northwest China, **Environmental Earth Sciences**, 73, 4671–4680, doi: 10.1007/s12665-014-3776-6, 2015.

Corneo, P. E., Kertesz, M. A., Bakhshandeh, S., Tahaei, H., Barbour, M. M., and Dijkstra, F. A.: Studying root water uptake of wheat genotypes in different soils using water $\delta^{18}O$ stable isotopes, **Agriculture, Ecosystems & Environment**, 264, 119-129, doi: 10.1016/j.agee.2018.05.007, 2018.

Craig, H. and Gordon, L. I.: Deuterium and oxygen 18 variations in the ocean and marine atmosphere, in: **Stable Isotopes in Oceanographic Studies and Paleotemperatures**, p. 9, 1965.

Cui, J., Tian, L., Wei, Z., Huntingford, C., Wang, P., Cai, Z., Ma, N., and Wang, L.: Quantifying the controls on evapotranspiration partitioning in the highest alpine meadow ecosystems, **Water Resources Research**, 56, doi: 10.1029/2019WR024815, 2020.

Draxler, R. R., and Hess, G.: Description of the HYSPLIT4 modeling system, **NOAA Tech Memo ERL ARL-224**, Dec, 24p., 1997.

Draxler, R. R.: Evaluation of an ensemble dispersion calculation, **Journal of Applied Meteorology**, 42, 308-317, doi: 10.1175/1520-0450(2003)042<0308:EOAEDC>2.0.CO;2, 2003.

Farquhar, G. D., and Cernusak, L. A.: On the isotopic composition of leaf water in the non-steady state, **Functional Plant Biology**, 32(4), 293-303, doi: 10.1071/FP04232, 2005.

Fiorella, R. P., Poulsen, C. J., and Matheny, A. M.: Seasonal patterns of water cycling in a deep, continental mountain valley inferred from stable water vapor isotopes, **Journal of Geophysical Research: Atmospheres**, 123, 7271-7291, doi: 10.1029/2017JD028093, 2018.

Flanagan, L. B., Comstock, J. P., and Ehleringer, J. R.: Comparison of modeled and observed environmental influences on the stable oxygen and hydrogen isotope composition of leaf water in Phaseolus vulgaris L, **Plant Physiology**, 96, 588-596, doi: https://doi.org/10.1104/pp.96.2.588, 1991.

Fricke, H. C., O'Neil, J. R. J. E., and Letters, P. S.: The correlation between $^{18}O/^{16}O$ ratios of meteoric water and surface temperature: its use in investigating terrestrial climate change over geologic time, **Earth and Planetary Science Letters**, 170, 181-196, doi: 10.1016/S0012-821X(99)00105-3, 1999.

Galewsky, J., Rella, C., Sharp, Z., Samuels, K., and Ward, D.: Surface measurements of upper tropospheric water vapor isotopic composition on the Chajnantor Plateau, Chile, **Geophysical Research Letters**, 38, 1-5, doi: 10.1029/2011GL048557, 2011.

Good, S. P., Soderberg, K., Wang, L., and Caylor, K. K.: Uncertainties in the assessment of the isotopic composition of surface fluxes: A direct comparison of techniques using laser-based water vapor isotope analyzers, **Journal of Geophysical Research: Atmospheres**, 117, doi: 10.1029/2011JD017168, 2012.

Griffis, T. J., Wood, J. D., Baker, J. M., Lee, X., Xiao, K., Chen, Z., Welp, L. R., Schultz, N. M., Gorski, G., and Chen, M.: Investigating the source, transport, and isotope composition of water vapor in the planetary boundary layer, **Atmospheric Chemistry and Physics**, 16, 5139-5157, doi: 10.5194/acp-16-5139-2016, 2016.

Hobbins, M. T., Ramirez, J. A., and Brown, T. C.: The complementary relationship in estimation of regional evapotranspiration: An enhanced advection-aridity model, **Water Resources Research**, 37, 1389-1403, doi: 10.1029/2000WR900359, 2001.

Jung, M., Reichstein, M., Ciais, P., Seneviratne, S. I., Sheffield, J., Goulden, M. L., Bonan, G., Cescatti, A., Chen, J., and De Jeu, R.: Recent decline in the global land evapotranspiration trend due to limited moisture supply, **Nature**, 467, 951-954, doi: 10.1038/nature09396, 2010.

Kaseke, K. F., Wang, L., Wanke, H., Tian, C., Lanning, M., and Jiao, W.: Precipitation origins and key drivers of precipitation isotope (^{18}O, ^{2}H, and ^{17}O) compositions over windhoek, **Journal of Geophysical Research: Atmospheres**, 123, 7311-7330, doi: 10.1029/2018JD028470, 2018.

Keeling, C. D.: The concentration and isotopic abundances of atmospheric carbon dioxide in rural areas, **Geochimica et Cosmochimica Acta**, 13, 322-334, doi: 10.1016/0016-7037(58)90033-4, 1958.

Keeling, C. D.: The concentration and isotopic abundances of carbon dioxide in rural and marine air, **Geochimica et Cosmochimica Acta**, 24, 277-298, doi: 10.1016/0016-7037(61)90023-0, 1961.

Keppler, F., Schiller, A., Ehehalt, R., Greule, M., Hartmann, J., and Polag, D.: Stable isotope and high precision concentration measurements confirm that all humans produce and exhale methane, **Journal of Breath Research**, 10, 016003, doi: 10.1088/1752-7155/10/1/016003, 2016.

Kerstel, E., and Gianfrani, L.: Advances in laser-based isotope ratio measurements: selected applications, **Applied Physics B**, 92, 439-449, doi: 10.1007/s00340-008-3128-x, 2008.

Kong, Y., Pang, Z., and Froehlich, K.: Quantifying recycled moisture fraction in precipitation of an arid region using deuterium excess, **Tellus B: Chemical and Physical Meteorology**, 65, 19251, doi: 10.3402/tellusb.v65i0.19251, 2013.

Lai, C.T., Ometto, J. P., Berry, J. A., Martinelli, L. A., Domingues, T. F., and Ehleringer, J. R.: Life form-specific variations in leaf water oxygen-18 enrichment in Amazonian vegetation, **Oecologia**, 157, 197-210, doi: 10.1007/s00442-008-1071-5, 2008.

Lanning, M., Wang, L., Benson, M., Zhang, Q., and Novick, K. A.: Canopy isotopic investigation reveals different water uptake dynamics of maples and oaks, **Phytochemistry**, 175, 112389, doi:10.1016/j.phytochem.2020.112389, 2020.

Li, Z., Feng, Q., Wang, Q., Kong, Y., Chen, A., Song, Y., Li, Y., Li, J., and Guo, X.: Contributions of local terrestrial evaporation and transpiration to precipitation using $\delta^{18}O$ and D-excess as a proxy in Shiyang inland river basin in China, **Global and Planetary Change**, 146, 140-151, doi: 10.1016/j.gloplacha.2016.10.003, 2016.

Lovie, P.: Coefficient of variation**, Encyclopedia of Statistics in Behavioral Science**, doi: 10.1002/0470013192.bsa107, 2005.

Ma, Q., Zhang, M., Wang, S., Wang, Q., Liu, W., Li, F., and Chen, F.: An investigation of moisture sources and secondary evaporation in Lanzhou, Northwest China, **Environmental Earth Sciences**, 71, 3375-3385, doi: 10.1007/s12665-013-2728-x, 2014.

Mahindawansha, A., Orlowski, N., Kraft, P., Rothfuss, Y., Racela, H., and Breuer, L.: Quantification of plant water uptake by water stable isotopes in rice paddy systems, **Plant and Soil**, 429, 281-302, doi: 10.1007/s11104-018-3693-7, 2018.

Majoube, M.: Fractionnement en oxygene 18 et en deuterium entre l'eau et sa vapeur, **Journal de Chimie Physique**, 68, 1423-1436, doi: 10.1051/jcp/1971681423, 1971.

Merlivat, L., and Jouzel, J.: Global climatic interpretation of the deuterium-oxygen 18 relationship for precipitation, **Journal of Geophysical Research: Oceans**, 84, 5029-5033, doi: 10.1029/JC084iC08p05029, 1979.

Miller, J. B., and Tans, P. P.: Calculating isotopic fractionation from atmospheric measurements at various scales, **Tellus B**, 55, 207-214, doi: 10.1034/j.1600-0889.2003.00020.x, 2003.

Moreira, M., Sternberg, L., Martinelli, L., Victoria, R., Barbosa, E., Bonates, L., and Nepstad, D.: Contribution of transpiration to forest ambient vapour based on isotopic measurements, **Global Change Biology**, 3, 439-450, doi: 10.1046/j.1365-2486.1997.00082.x, 1997.

Parkes, S., McCabe, M., Griffiths, A. D., Wang, L., Chambers, S., Ershadi, A., Williams, A. G., Strauss, J., and Element, A.: Response of water vapour D-excess to land-atmosphere interactions in a semi-arid environment, **Hydrolgy and Earth System Sciences**, 21, 533–548, doi:10.5194/hess-21-533-2017, 2016.

Peng, T. R., Liu, K. K., Wang, C. H., and Chuang, K. H.: A water isotope approach to assessing moisture recycling in the island-based precipitation of Taiwan: A case study in the western Pacific, **Water Resources Research**, 47, W08507, doi: 10.1029/2010WR009890, 2011.

Seneviratne, S. I., Lüthi, D., Litschi, M., and Schär, C.: Land–atmosphere coupling and climate change in Europe, **Nature**, 443, 205-209, doi: 10.1038/nature05095, 2006.

Song, X., Barbour, M. M., Saurer, M., and Helliker, B. R.: Examining the large-scale convergence of photosynthesis-weighted tree leaf temperatures through stable oxygen isotope analysis of multiple data sets, **New Phytologist**, 192: 912–924, doi: 10.1111/j.1469-8137.2011.03851.x, 2011.

Song, X., Simonin, K. A., Loucos, K. E., and Barbour, M. M.: Modelling non-steady-state isotope enrichment of leaf water in a gas-exchange cuvette environment, **Plant, Cell & Environment**, 38, 2618-2628, doi: 10.1111/pce.12571, 2015.

Steen-Larsen, H. C., Johnsen, S. J., Masson-Delmotte, V., Stenni, B., Risi, C., Sodemann, H., Balslev-Clausen, D., Blunier, T., Dahl-Jensen, D., and Ellehøj, M. D.: Continuous monitoring of summer surface water vapor isotopic composition above the Greenland Ice Sheet, **Atmospheric Chemistry and Physics**, 13, 4815-4828, doi:10.5194/acp-13-4815-2013, 2013.

Stein, A., Draxler, R. R., Rolph, G. D., Stunder, B. J., Cohen, M., and Ngan, F.: NOAA's HYSPLIT atmospheric transport and dispersion modeling system, **Bulletin of the American Meteorological Society**, 96, 2059-2077, doi: 10.1175/BAMS-D-14-00110.1, 2015.

Trenberth, K. E.: Atmospheric moisture recycling: Role of advection and local evaporation, **Journal of Climate**, 12, 1368-1381, doi: 10.1175/15200442(1999)012<1368:AMRROA>2.0.CO;2, 1999.

Unger, S., Máguas, C., Pereira, J. S., Aires, L. M., David, T. S., and Werner, C.: Disentangling drought-induced variation in ecosystem and soil respiration using stable carbon isotopes, **Oecologia**, 163, 1043-1057, doi: 10.1007/s00442-010-1576-6, 2010.

Wagle, P., Skaggs, T. H., Gowda, P. H., Northup, B. K., and Neel, J. P.: Flux variance similarity-based partitioning of evapotranspiration over a rainfed alfalfa field using high frequency eddy covariance data, **Agricultural and Forest Meteorology**, 285, 107907, doi: 10.1016/j.agrformet.2020.107907, 2020.

Wang, L., Caylor, K. K., and Dragoni, D.: On the calibration of continuous, high-precision $\delta^{18}O$ and $\delta^{2}H$ measurements using an off-axis integrated cavity output spectrometer, **Rapid Communications in Mass Spectrometry**, 23, 530-536, doi: 10.1002/rcm.3905, 2009.

Wang, L., Caylor, K. K., Villegas, J. C., Barron-Gafford, G. A., Breshears, D. D., and Huxman, T. E.: Partitioning evapotranspiration across gradients of woody plant cover: Assessment of a stable isotope technique, **Geophysical Research Letters**, 37, L09401, doi: 10.1029/2010GL043228, 2010.

Wang, L., Good, S. P., Caylor, K. K., and Cernusak, L. A.: Direct quantification of leaf transpiration isotopic composition, **Agricultural and Forest Meteorology**, 154-155, 127-135, doi: 10.1016/j.agrformet.2011.10.018, 2012.

Wang, L., Niu, S., Good, S. P., Soderberg, K., McCabe, M. F., Sherry, R. A., Luo, Y., Zhou, X., Xia, J., and Caylor, K. K.: The effect of warming on grassland evapotranspiration partitioning using laser-based isotope monitoring techniques, **Geochimica et Cosmochimica Acta**, 111, 28-38, doi: 10.1016/j.gca.2012.12.047, 2013.

Wang, L., Good, S. P., and Caylor, K. K.: Global synthesis of vegetation control on evapotranspiration partitioning, **Geophysical Research Letters**, 41, 6753–6757, 10.1002/2014GL061439, 2014.

Wei, Z., Yoshimura, K., Okazaki, A., Kim, W., Liu, Z., and Yokoi, M.: Partitioning of evapotranspiration using high-frequency water vapor isotopic measurement over a rice paddy field, **Water Resources Research**, 51, 3716-3729, doi: 10.1002/2014WR016737, 2015.

Werner, M., Langebroek, P. M., Carlsen, T., Herold, M., and Lohmann, G.: Stable water isotopes in the ECHAM5 general circulation model: Toward high-resolution isotope modeling on a global scale, **Journal of Geophysical Research: Atmospheres**, 116, D15109, doi:10.1029/2011JD015681, 2011.

Yakir, D., and Wang, X.F.: Fluxes of CO_2 and water between terrestrial vegetation and the atmosphere estimated from isotope measurements, **Nature**, 380, 515-517, doi: 10.1038/380515a0, 1996.

Yakir, D., and Sternberg, L.: The use of stable isotopes to study ecosystem gas exchange, **Oecologia**, 123, 297-311, doi: 10.1007/s004420051016, 2000.

Yamanaka, T., and Shimizu, R.: Spatial distribution of deuterium in atmospheric water vapor: Diagnosing sources and the mixing of atmospheric moisture, **Geochimica et Cosmochimica Acta**, 71, 3162-3169, doi: 10.1016/j.gca.2007.04.014, 2007.

Yepez, E. A., Williams, D. G., Scott, R. L., and Lin, G.: Partitioning overstory and understory evapotranspiration in a semiarid savanna woodland from the isotopic composition of water vapor, **Agricultural and Forest Meteorology**, 119, 53-68, doi: 10.1016/S0168-1923(03)00116-3, 2003.

Zhang, L., Dawes, W., and Walker, G.: Response of mean annual evapotranspiration to vegetation changes at catchment scale, **Water Resources Research**, 37, 701-708, doi: 10.1029/2000WR900325, 2001.

Zhang, Y., Shen, Y., Sun, H., and Gates, J. B.: Evapotranspiration and its partitioning in an irrigated winter wheat field: A combined isotopic and micrometeorologic approach, **Journal of Hydrology**, 408, 203-211, doi: 10.1016/j.jhydrol.2011.07.036, 2011.

Zhao, L., Liu, X., Wang, N., Kong, Y., Song, Y., He, Z., Liu, Q., and Wang, L.: Contribution of recycled moisture to local precipitation in the inland Heihe River Basin, **Agricultural and Forest Meteorology**, 271, 316-335, doi: 10.1016/j.agrformet.2019.03.014, 2019.

Zhu, G., Guo, H., Qin, D., Pan, H., Zhang, Y., Jia, W., and Ma, X.: Contribution of recycled moisture to precipitation in the monsoon marginal zone: Estimate based on stable isotope data, **Journal of Hydrology**, 569, 423-435, doi: 10.1016/j.jhydrol.2018.12.014, 2019.

11. Appendix

Proposition. In the traditional linear Keeling plot system, denote $\delta_a = f(t)$, $\delta_v = g(t)$, $\delta_{ET} = h(t)$ and $C_a = I(t) > 0$ as continuous functions of time. And for two definite moments t_1 and t_2 ($t_1 < t_2$), $\delta_{a_1} \neq \delta_{a_2} \neq \delta_{v_1} \neq \delta_{v_2} \neq \delta_{ET_1} \neq \delta_{ET_2}$. The slopes of corresponding keeling plot curve are $k_1 = C_{a_1}(\delta_{a_1} - \delta_{ET_1})$ and $k_2 = C_{a_2}(\delta_{a_2} - \delta_{ET_2})$, respectively. Then we have that when $k_1 k_2 < 0$, there exists $[t_1', t_2'] \subset [t_1, t_2]$, such that $[min(f(t_1'), f(t_2')), max(f(t_1'), f(t_2'))] \subset [min(\delta_{v_1}, \delta_{v_2}), max(\delta_{v_1}, \delta_{v_2})]$.

Remark: To make a proof of the proposition, classical Intermediate Value Theorem (IVT) was used. It states that if f is a continuous function from the interval $I = [a, b]$ to real number (R). Then *Version I.* if u is a number between $f(a)$ and $f(b)$, there is *c* in (a, b) such that $f(c) = u$. *Version II.* the image set $f(I)$ is also an interval, and it contains $[min(f(a), f(b)), max(f(a), f(b))]$. While in this study, IVT was able to be explained as follows: if f is a continuous function from the interval $I = [t_1, t_2]$ to R with $min[f(t_1), f(t_2)] < \delta_v$ and $max[f(t_1), f(t_2)] > \delta_v$, then *Version I* implies that there is $t' \in (t_1, t_2)$ such that $f(t') = \delta_v$. And *Version II* implies that the image set $f(I)$ is also an interval, and it contains $[min(f(t_1), f(t_2)), max(f(t_1), f(t_2))]$.

Proof. Since $k_1 k_2 < 0$, we have $\delta_{a_1} < \delta_{v_1}$ and $\delta_{a_2} > \delta_{v_2}$, or $\delta_{a_1} > \delta_{v_1}$ and $\delta_{a_2} < \delta_{v_2}$. As a result, the cases $\delta_{a_1} < \delta_{v_1} < \delta_{a_2} < \delta_{v_2}$, $\delta_{v_1} < \delta_{a_1} < \delta_{v_2} < \delta_{a_2}$, $\delta_{v_2} < \delta_{a_2} < \delta_{v_1} < \delta_{a_1}$, $\delta_{a_2} < \delta_{v_2} < \delta_{a_1} < \delta_{v_1}$ and $[min(\delta_{v_1}, \delta_{v_2}), max(\delta_{v_1}, \delta_{v_2})] \cap [min(\delta_{a_1}, \delta_{a_2}), max(\delta_{a_1}, \delta_{a_2})] = \emptyset$ do not meet the precondition $k_1 k_2 < 0$. There are only four cases below. We will prove the proposition in each of the four cases.

Case 1: $[min(\delta_{v_1}, \delta_{v_2}), max(\delta_{v_1}, \delta_{v_2})] \subset [min(\delta_{a_1}, \delta_{a_2}), max(\delta_{a_1}, \delta_{a_2})]$ **(Fig. 1 a)**.

Formatted: Font: Bold

Deleted:):

Formatted: Font: Bold

According to IVT *Version I*, there exists $t_1' \in [t_1, t_2]$, such that $f(t_1') = \delta_{v_1}$; similarly, there exists $t_2' \in [t_1, t_2]$, such that $f(t_2') = \delta_{v_2}$. Based on IVT *Version II*, there exists $[t_1', t_2'] \subset [t_1, t_2]$, such that $[min(f(t_1'), f(t_2')), max(f(t_1'), f(t_2'))] = [min(\delta_{v_1}, \delta_{v_2}), max(\delta_{v_1}, \delta_{v_2})]$.

Case 2: $[min(\delta_{a_1}, \delta_{a_2}), max(\delta_{a_1}, \delta_{a_2})] \subset [min(\delta_{v_1}, \delta_{v_2}), max(\delta_{v_1}, \delta_{v_2})]$ **(Fig. 1 b)**.

According to IVT *Version I*, there exists $t_1' \in [t_1, t_2]$, such that $f(t_1') = \delta_{a_1}$; similarly, there exists $t_2' \in [t_1, t_2]$, such that $f(t_2') = \delta_{a_2}$. Based on IVT *Version II*, there exists $[t_1', t_2'] \subset [t_1, t_2]$, such that $[min(f(t_1'), f(t_2')), max(f(t_1'), f(t_2'))] = [min(\delta_{a_1}, \delta_{a_2}), max(\delta_{a_1}, \delta_{a_2})] \subset [min(\delta_{v_1}, \delta_{v_2}), max(\delta_{v_1}, \delta_{v_2})]$.

Case 3: $\delta_{v_2} < \delta_{a_1} < \delta_{v_1} < \delta_{a_2}$, or $\delta_{a_2} < \delta_{v_1} < \delta_{a_1} < \delta_{v_2}$ **(Fig. 1 c and Fig. 1 d)**.

According to IVT Version I, there exists $t_2' \in [t_1, t_2]$, such that $f(t_2') = \delta_{v_1}$. Given case (2), when $[\min(\delta_{a_1}, \delta_{v_1}), \max(\delta_{a_1}, \delta_{v_1})] \subset [min(\delta_{v_1}, \delta_{v_2}), max(\delta_{v_1}, \delta_{v_2})]$, there exists $[t_1', t_2'] \subset [t_1, t_2'] \subset [t_1, t_2]$, such that $[min(f(t_1'), f(t_2')), max(f(t_1'), f(t_2'))] \subset [min(\delta_{a_1}, \delta_{v_1}), max(\delta_{a_1}, \delta_{v_1})] \subset [min(\delta_{v_1}, \delta_{v_2}), max(\delta_{v_1}, \delta_{v_2})]$.

Case 4: $\delta_{v_1} < \delta_{a_2} < \delta_{v_2} < \delta_{a_1}$, or $\delta_{a_1} < \delta_{v_2} < \delta_{a_2} < \delta_{v_1}$ **(Fig. 1 e and Fig.1 f)**.

According to IVT Version I, there exists $t_1' \in [t_1, t_2]$, such that $f(t_1') = \delta_{v_2}$. Based on case (2), when $[\min(\delta_{a_2}, \delta_{v_2}), \max(\delta_{a_2}, \delta_{v_2})] \subset [min(\delta_{v_1}, \delta_{v_2}), max(\delta_{v_1}, \delta_{v_2})]$, there exists $[t_1', t_2'] \subset [t_1', t_2] \subset [t_1, t_2]$, such that $[min(f(t_1'), f(t_2')), max(f(t_1'), f(t_2'))] \subset [min(\delta_{a_2}, \delta_{v_2}), max(\delta_{a_2}, \delta_{v_2})] \subset [min(\delta_{v_1}, \delta_{v_2}), max(\delta_{v_1}, \delta_{v_2})]$.

Thus the proposition is true for all four possible scenarios, which make the estimation of δ_a theoretically feasibly when $k_1 k_2 < 0$ and δ_{v_1} and δ_{v_2} adequately close. Actual δ_a between t_1 and t_2 can be ensured in the interval $[min(\delta_{v_1}, \delta_{v_2}), max(\delta_{v_1}, \delta_{v_2})]$.

Deleted: For convenience, we denote $A = [min(f(t_1'), f(t_2')), max(f(t_1'), f(t_2'))]$, and $B = [min(\delta_{v_1}, \delta_{v_2}), max(\delta_{v_1}, \delta_{v_2})]$.

Formatted: Font: Italic

Deleted: *A*

Deleted: *B*

Deleted:

Formatted: Font: Bold

Deleted:):

Formatted: Font: Bold

Formatted: Font: Italic

Deleted: For convenience, we denote $A = [min(f(t_1'), f(t_2')), max(f(t_1'), f(t_2'))]$, and $B = [min(\delta_{v_1}, \delta_{v_2}), max(\delta_{v_1}, \delta_{v_2})]$.

Formatted: Font: Italic

Deleted:

Deleted: *A*

Deleted: *B*

Deleted:):

Formatted: Font: Bold

Deleted: t

Deleted: *A*

Deleted: *B*

Deleted: (For convenience, we denote $A = [min(f(t_1'), f(t_2')), max(f(t_1'), f(t_2'))]$, and $B = [min(\delta_{v_1}, \delta_{v_2}), max(\delta_{v_1}, \delta_{v_2})]$).

Formatted: Font: Bold

Deleted: :

Deleted:

Deleted: *A*

Deleted: *B*(For convenience, we denote $A = [min(f(t_1'), f(t_2')), max(f(t_1'), f(t_2'))]$, and $B = [min(\delta_{v_1}, \delta_{v_2}), max(\delta_{v_1}, \delta_{v_2})]$). ¶

To simplify the result, actual δ_a between t_1 and t_2 can be approximately regarded as what Eq. (7) reveals.

Deleted: Page Break
¶

Formatted: Justified, Indent: First line: 0"

Table 1. The number of estimated isotope composition of ambient vapor meeting the criteria using the intersection point method ($\delta_{a(IP)}$) and the Intermediate Value Theorem method ($\delta_{a(IVT)}$) among all 49 days.

Date	number of $\delta_{a\,(IP)}$ values meeting the criteria in a whole day	number of $\delta_{a\,(IVT)}$ values meeting the criteria in a whole day
5/19	27	8
5/27	13	3
5/28	30	3
5/31	25	5
6/4	38	5
6/5	28	0
6/7	29	6
6/9	32	5
6/10	26	2
6/11	21	4
6/12	22	4
6/15	32	0
6/16	33	0
6/17	24	1
6/18	26	0
6/21	26	3
6/22	22	0
6/26	22	0
6/27	29	3
7/4	23	0
7/5	23	1
7/7	30	0
7/8	29	0
7/14	28	4
7/16	28	0
7/18	25	1
7/19	28	6
7/20	27	6
7/21	29	0
7/22	19	0
8/3	18	1
8/4	22	3
8/5	25	3
8/6	28	1
8/12	13	8
8/18	19	3
8/19	30	0
8/28	23	0
8/29	22	1
8/30	27	1
8/31	27	0
9/20	25	0
9/21	24	1
9/22	31	1
9/23	28	1
9/27	28	2
9/28	25	1
9/29	30	5
9/30	25	1

Formatted: Font: (Default) +Body (Times New Roman), Font color: Auto

Formatted: Line spacing: single

Formatted: Font: (Default) +Body (Times New Roman), Font color: Auto

Formatted: Centered, Indent: Left: 0", First line: 0"

Formatted: Check spelling and grammar

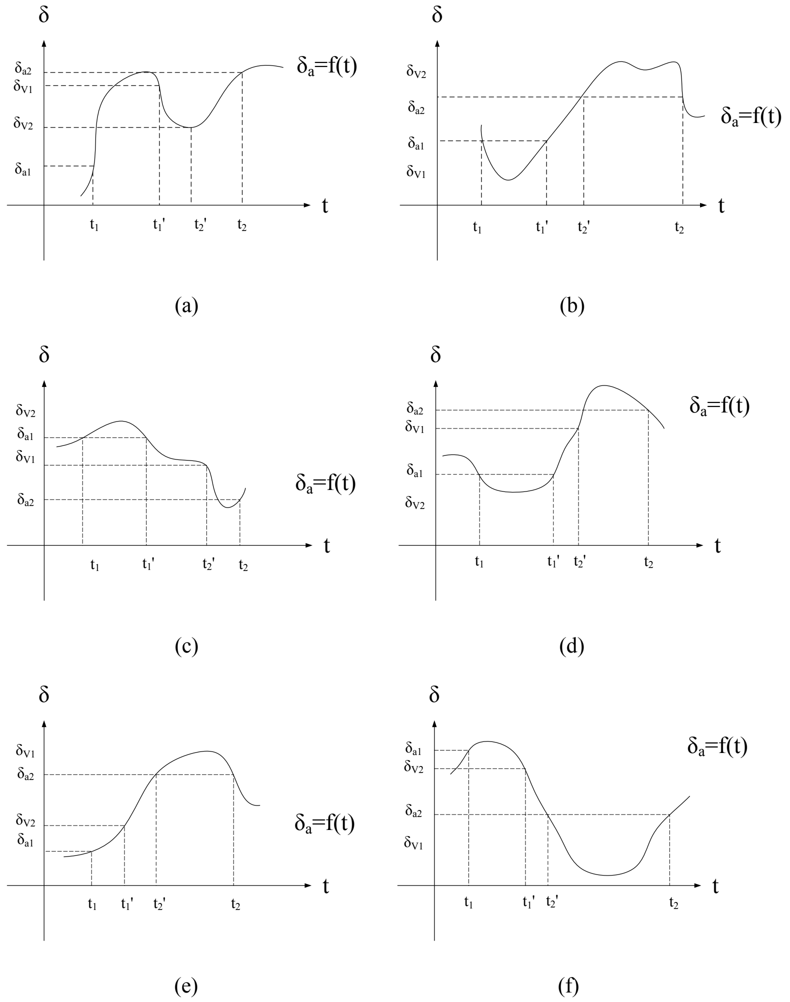

Fig. 1 Theoretical diagrams of all possible combinations of the relationships between isotope composition of ambient vapor (δ_a) and observed isotope composition of atmospheric vapor (δ_v) of two continuous moments t_1 and t_2, ($t_1 < t_2$). δ_{a1} and δ_{a2} represent δ_a value in t_1 and t_2, respectively. δ_{v1} and δ_{v2} represent δ_v value in t_1 and t_2, respectively. t_1' and t_2' represent the time of two specific moments between t_1 and t_2 with $t_1 < t_1' < t_2' < t_2$. For all of the six situations, there exists some sub-intervals $[t_1', t_2'] \subset [t_1, t_2]$ such that the whole range of $\{\delta_a(t): t \in [t_1', t_2']\}$ is within $[min(\delta_{v_1}, \delta_{v_2}), max(\delta_{v_1}, \delta_{v_2})]$.

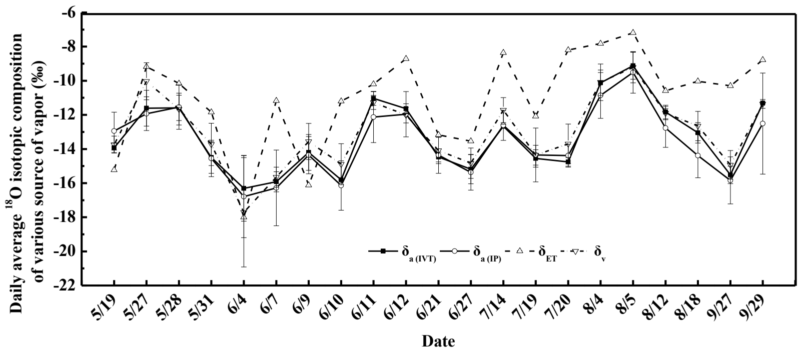

Fig. 2 The daily average values of the isotope composition of evapotranspiration vapor (δ_{ET}), the isotope composition of atmospheric vapor (δ_v), the estimated isotope composition of ambient vapor using the intersection point method ($\delta_{a(IP)}$) and the Intermediate Value Theorem method ($\delta_{a(IVT)}$) in the 21 days (see method section 2.3).

Formatted: Font color: Auto

Formatted: Font color: Auto

Formatted: Font color: Auto

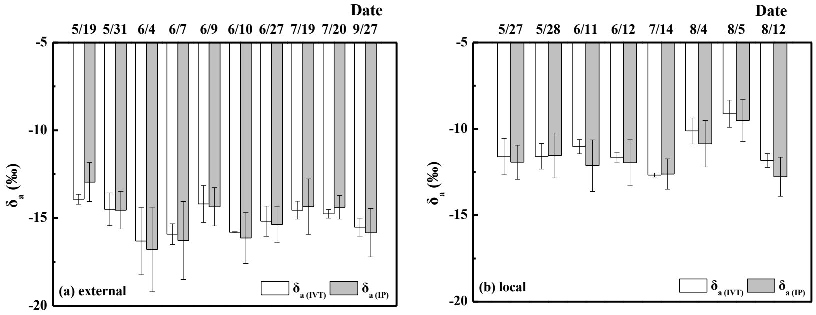

Fig. 3 The daily average values of the estimated isotope composition of ambient vapor using the intersection point method ($\delta_{a(IP)}$) and the Intermediate Value Theorem method ($\delta_{a(IVT)}$) after filter. Hybrid Single Particle Lagrangian Integrated Trajectory (HYSPLIT) backward trajectory showed external origin (a) and local origin (b), respectively.

Formatted: Font color: Auto

Formatted: Justified, Indent: First line: 0", Line spacing: single

Formatted: Font color: Auto

Formatted: Justified, Indent: First line: 0", Line spacing: single, Tab stops: Not at 5.14"

Formatted: Font color: Auto

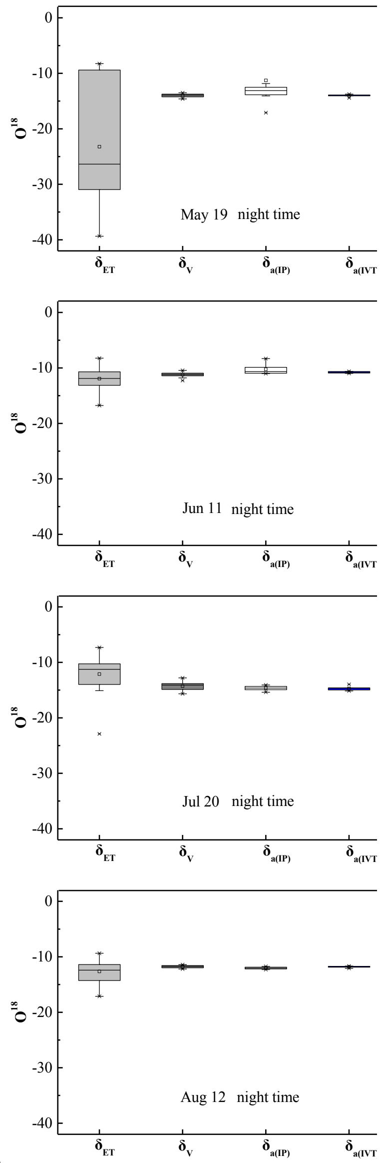

Deleted:

... [45]

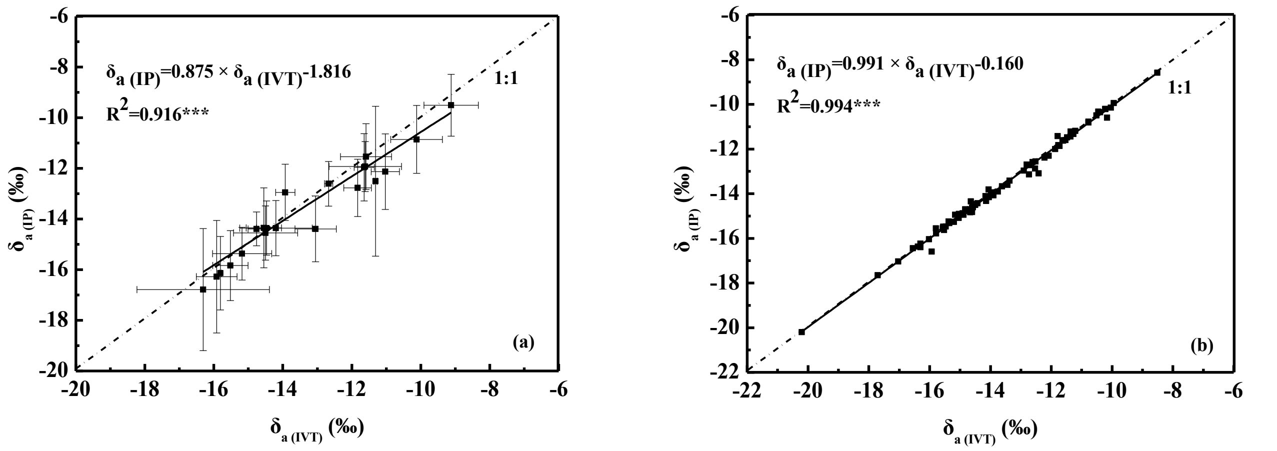

Fig. 4 Linear regression between the estimated isotope composition of ambient vapor using the intersection point method ($\delta_{a(IP)}$) and the Intermediate Theorem method ($\delta_{a(IVT)}$) on daily scale (a) and point to point scale (b), respectively.

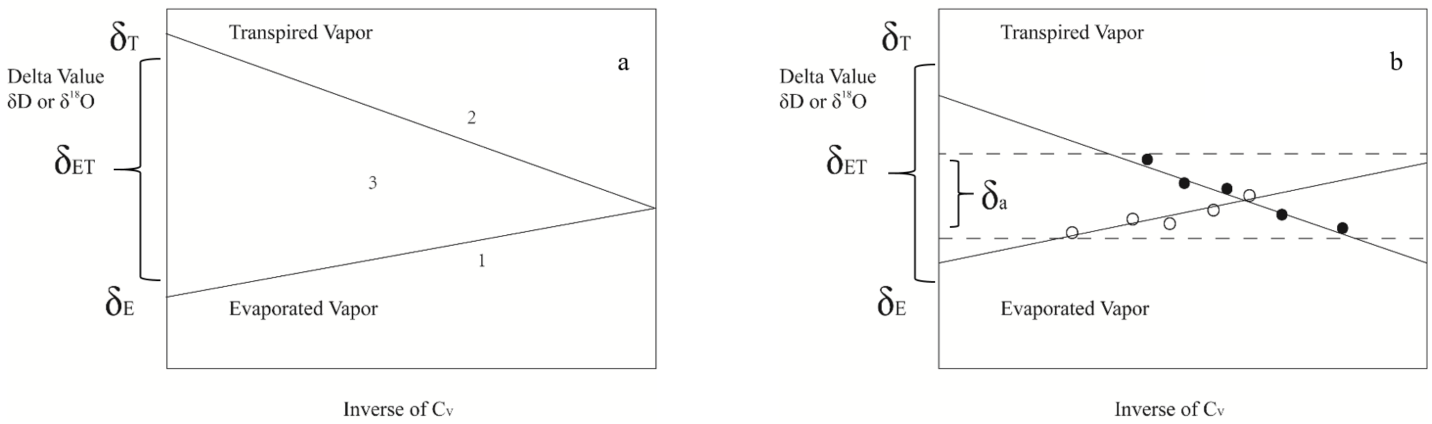

Fig. 5 Hypothetical graph of the idealized Keeling plot curve of the isotope composition of evaporation vapor (δ_E) curve (line 1), the isotope composition of transpiration vapor (δ_T) curve (line 2) and the isotope composition of evapotranspiration vapor (δ_{ET}) curve (area 3) (a), and hypothetical graph of idealized δ_E, δ_T lines and the interval of possible the isotope composition of ambient vapor (δ_a) in the Keeling plots (b).

Page 3: [1] Deleted	**Yusen Yuan**	**4/27/20 4:20:00 PM**
Page 3: [1] Deleted	**Yusen Yuan**	**4/27/20 4:20:00 PM**
Page 3: [2] Deleted	**LW**	**5/1/20 1:30:00 PM**
Page 3: [2] Deleted	**LW**	**5/1/20 1:30:00 PM**
Page 3: [2] Deleted	**LW**	**5/1/20 1:30:00 PM**
Page 3: [2] Deleted	**LW**	**5/1/20 1:30:00 PM**
Page 3: [2] Deleted	**LW**	**5/1/20 1:30:00 PM**
Page 3: [2] Deleted	**LW**	**5/1/20 1:30:00 PM**
Page 3: [3] Deleted	**Yusen Yuan**	**2/18/20 6:13:00 PM**
Page 3: [4] Deleted	**Yusen Yuan**	**4/27/20 3:23:00 AM**
Page 3: [4] Deleted	**Yusen Yuan**	**4/27/20 3:23:00 AM**
Page 3: [5] Deleted	**LW**	**5/1/20 1:32:00 PM**
Page 3: [5] Deleted	**LW**	**5/1/20 1:32:00 PM**

Page 3: [6] Deleted	Yusen Yuan	4/27/20 3:40:00 PM

Page 3: [6] Deleted	Yusen Yuan	4/27/20 3:40:00 PM

Page 3: [7] Formatted	Yusen Yuan	4/27/20 4:20:00 PM

Font color: Blue

Page 3: [7] Formatted	Yusen Yuan	4/27/20 4:20:00 PM

Font color: Blue

Page 3: [8] Deleted	LW	5/1/20 2:35:00 PM

Page 3: [9] Formatted	Yusen Yuan	4/10/20 12:48:00 AM

Font color: Auto

Page 3: [9] Formatted	Yusen Yuan	4/10/20 12:48:00 AM

Font color: Auto

Page 3: [9] Formatted	Yusen Yuan	4/10/20 12:48:00 AM

Font color: Auto

Page 3: [9] Formatted	Yusen Yuan	4/10/20 12:48:00 AM

Font color: Auto

Page 3: [10] Formatted	Yusen Yuan	4/10/20 12:48:00 AM

Font color: Auto

Page 3: [10] Formatted	Yusen Yuan	4/10/20 12:48:00 AM

Font color: Auto

Page 3: [11] Deleted	Yusen Yuan	5/7/20 10:53:00 PM

Page 3: [11] Deleted	Yusen Yuan	5/7/20 10:53:00 PM

Page 3: [11] Deleted	**Yusen Yuan**	**5/7/20 10:53:00 PM**

Page 9: [12] Deleted	**LW**	**4/14/20 9:17:00 AM**

Page 9: [12] Deleted	**LW**	**4/14/20 9:17:00 AM**

Page 9: [12] Deleted	**LW**	**4/14/20 9:17:00 AM**

Page 9: [12] Deleted	**LW**	**4/14/20 9:17:00 AM**

Page 9: [12] Deleted	**LW**	**4/14/20 9:17:00 AM**

Page 9: [12] Deleted	**LW**	**4/14/20 9:17:00 AM**

Page 9: [12] Deleted	**LW**	**4/14/20 9:17:00 AM**

Page 9: [12] Deleted	**LW**	**4/14/20 9:17:00 AM**

Page 9: [12] Deleted	**LW**	**4/14/20 9:17:00 AM**

Page 9: [12] Deleted	**LW**	**4/14/20 9:17:00 AM**

Page 9: [12] Deleted	**LW**	**4/14/20 9:17:00 AM**

Page 9: [12] Deleted	**LW**	**4/14/20 9:17:00 AM**

Page 9: [12] Deleted	LW	4/14/20 9:17:00 AM

Page 9: [13] Formatted	LW	5/9/20 10:42:00 PM

Not Highlight

Page 9: [13] Formatted	LW	5/9/20 10:42:00 PM

Not Highlight

Page 9: [14] Formatted	LW	5/9/20 10:42:00 PM

Not Highlight

Page 9: [14] Formatted	LW	5/9/20 10:42:00 PM

Not Highlight

Page 9: [15] Deleted	LW	5/9/20 4:22:00 PM

Page 9: [15] Deleted	LW	5/9/20 4:22:00 PM

Page 9: [15] Deleted	LW	5/9/20 4:22:00 PM

Page 9: [15] Deleted	LW	5/9/20 4:22:00 PM

Page 9: [15] Deleted	LW	5/9/20 4:22:00 PM

Page 9: [15] Deleted	LW	5/9/20 4:22:00 PM

Page 9: [15] Deleted	LW	5/9/20 4:22:00 PM

Page 9: [15] Deleted	LW	5/9/20 4:22:00 PM

Page 9: [15] Deleted	LW	5/9/20 4:22:00 PM

Page 9: [15] Deleted	LW	5/9/20 4:22:00 PM

Page 10: [16] Deleted	Yusen Yuan	5/7/20 4:05:00 AM

Page 10: [16] Deleted	Yusen Yuan	5/7/20 4:05:00 AM

Page 10: [17] Formatted	Yusen Yuan	4/8/20 8:10:00 PM

Superscript

Page 10: [17] Formatted	Yusen Yuan	4/8/20 8:10:00 PM

Superscript

Page 10: [17] Formatted	Yusen Yuan	4/8/20 8:10:00 PM

Superscript

Page 10: [18] Deleted	LW	4/13/20 11:11:00 PM

Page 10: [18] Deleted	LW	4/13/20 11:11:00 PM

Page 10: [18] Deleted	LW	4/13/20 11:11:00 PM

Page 10: [19] Deleted	Yusen Yuan	4/9/20 1:33:00 AM

Page 10: [19] Deleted	Yusen Yuan	4/9/20 1:33:00 AM

Page 10: [19] Deleted **Yusen Yuan** **4/9/20 1:33:00 AM**

Page 10: [20] Formatted **Yusen Yuan** **4/9/20 1:52:00 AM**

Font: (Asian) +Body Asian (SimSun), Font color: Auto

Page 10: [20] Formatted **Yusen Yuan** **4/9/20 1:52:00 AM**

Font: (Asian) +Body Asian (SimSun), Font color: Auto

Page 10: [21] Deleted **LW** **4/14/20 10:51:00 AM**

Page 10: [21] Deleted **LW** **4/14/20 10:51:00 AM**

Page 10: [21] Deleted **LW** **4/14/20 10:51:00 AM**

Page 10: [22] Deleted **Yusen Yuan** **4/9/20 2:02:00 AM**

Page 10: [22] Deleted **Yusen Yuan** **4/9/20 2:02:00 AM**

Page 10: [22] Deleted **Yusen Yuan** **4/9/20 2:02:00 AM**

Page 10: [22] Deleted **Yusen Yuan** **4/9/20 2:02:00 AM**

Page 10: [22] Deleted **Yusen Yuan** **4/9/20 2:02:00 AM**

Page 10: [22] Deleted **Yusen Yuan** **4/9/20 2:02:00 AM**

Page 10: [22] Deleted	Yusen Yuan	4/9/20 2:02:00 AM

Page 10: [22] Deleted	Yusen Yuan	4/9/20 2:02:00 AM

Page 10: [22] Deleted	Yusen Yuan	4/9/20 2:02:00 AM

Page 10: [22] Deleted	Yusen Yuan	4/9/20 2:02:00 AM

Page 10: [22] Deleted	Yusen Yuan	4/9/20 2:02:00 AM

Page 10: [22] Deleted	Yusen Yuan	4/9/20 2:02:00 AM

Page 10: [22] Deleted	Yusen Yuan	4/9/20 2:02:00 AM

Page 10: [22] Deleted	Yusen Yuan	4/9/20 2:02:00 AM

Page 10: [22] Deleted	Yusen Yuan	4/9/20 2:02:00 AM

Page 10: [22] Deleted	Yusen Yuan	4/9/20 2:02:00 AM

Page 10: [22] Deleted	Yusen Yuan	4/9/20 2:02:00 AM

Page 10: [22] Deleted	Yusen Yuan	4/9/20 2:02:00 AM

Page 10: [22] Deleted	Yusen Yuan	4/9/20 2:02:00 AM

Page 10: [22] Deleted	Yusen Yuan	4/9/20 2:02:00 AM

Page 10: [22] Deleted	Yusen Yuan	4/9/20 2:02:00 AM

Page 10: [22] Deleted	Yusen Yuan	4/9/20 2:02:00 AM

Page 10: [22] Deleted	Yusen Yuan	4/9/20 2:02:00 AM

Page 10: [22] Deleted	Yusen Yuan	4/9/20 2:02:00 AM

Page 10: [23] Formatted	Yusen Yuan	4/9/20 7:06:00 PM

Superscript

Page 10: [23] Formatted	Yusen Yuan	4/9/20 7:06:00 PM

Superscript

Page 10: [23] Formatted	Yusen Yuan	4/9/20 7:06:00 PM

Superscript

Page 10: [24] Deleted	Yusen Yuan	4/9/20 6:54:00 PM

Page 10: [24] Deleted	Yusen Yuan	4/9/20 6:54:00 PM

Page 10: [24] Deleted	Yusen Yuan	4/9/20 6:54:00 PM

Page 10: [25] Deleted	LW	4/14/20 11:03:00 AM

Page 10: [25] Deleted	LW	4/14/20 11:03:00 AM

Page 11: [26] Deleted	LW	4/14/20 11:02:00 AM

Page 11: [26] Deleted	LW	4/14/20 11:02:00 AM

Page 11: [26] Deleted	LW	4/14/20 11:02:00 AM

Page 11: [26] Deleted	LW	4/14/20 11:02:00 AM

Page 11: [26] Deleted	LW	4/14/20 11:02:00 AM

Page 11: [26] Deleted	LW	4/14/20 11:02:00 AM

Page 11: [26] Deleted	LW	4/14/20 11:02:00 AM

Page 11: [27] Formatted	Yusen Yuan	4/10/20 12:37:00 AM

Font color: Auto

Page 11: [27] Formatted	Yusen Yuan	4/10/20 12:37:00 AM

Font color: Auto

Page 11: [27] Formatted	Yusen Yuan	4/10/20 12:37:00 AM

Font color: Auto

Page 11: [27] Formatted	Yusen Yuan	4/10/20 12:37:00 AM

Font color: Auto

Page 11: [28] Deleted	LW	4/14/20 11:04:00 AM

Page 11: [28] Deleted	LW	4/14/20 11:04:00 AM

Page 11: [29] Deleted	Yusen Yuan	4/9/20 7:36:00 PM

Page 11: [29] Deleted	Yusen Yuan	4/9/20 7:36:00 PM

Page 11: [30] Deleted	LW	5/1/20 3:15:00 PM

Page 11: [30] Deleted	LW	5/1/20 3:15:00 PM

Page 11: [31] Deleted	Yusen Yuan	4/9/20 7:37:00 PM

Page 11: [32] Deleted	Yusen Yuan	4/9/20 7:39:00 PM

Page 11: [32] Deleted	Yusen Yuan	4/9/20 7:39:00 PM

Page 11: [32] Deleted	Yusen Yuan	4/9/20 7:39:00 PM

Page 11: [32] Deleted	Yusen Yuan	4/9/20 7:39:00 PM

Page 11: [32] Deleted	Yusen Yuan	4/9/20 7:39:00 PM

Page 11: [33] Deleted	Yusen Yuan	4/9/20 7:55:00 PM

Page 11: [33] Deleted	Yusen Yuan	4/9/20 7:55:00 PM

Page 11: [34] Deleted	LW	4/14/20 11:29:00 AM

Page 11: [34] Deleted	**LW**	**4/14/20 11:29:00 AM**

Page 11: [34] Deleted	**LW**	**4/14/20 11:29:00 AM**

Page 11: [34] Deleted	**LW**	**4/14/20 11:29:00 AM**

Page 11: [34] Deleted	**LW**	**4/14/20 11:29:00 AM**

Page 11: [35] Deleted	**LW**	**4/14/20 11:29:00 AM**

Page 11: [35] Deleted	**LW**	**4/14/20 11:29:00 AM**

Page 11: [35] Deleted	**LW**	**4/14/20 11:29:00 AM**

Page 11: [36] Deleted	**LW**	**4/14/20 11:29:00 AM**

Page 11: [36] Deleted	**LW**	**4/14/20 11:29:00 AM**

Page 11: [36] Deleted	**LW**	**4/14/20 11:29:00 AM**

Page 11: [36] Deleted	**LW**	**4/14/20 11:29:00 AM**

Page 11: [37] Deleted	**Yusen Yuan**	**4/9/20 7:54:00 PM**

Page 11: [38] Deleted	**Yusen Yuan**	**4/9/20 8:03:00 PM**

Page 11: [38] Deleted	Yusen Yuan	4/9/20 8:03:00 PM

Page 11: [38] Deleted	Yusen Yuan	4/9/20 8:03:00 PM

Page 11: [38] Deleted	Yusen Yuan	4/9/20 8:03:00 PM

Page 11: [39] Deleted	LW	4/14/20 11:30:00 AM

Page 11: [39] Deleted	LW	4/14/20 11:30:00 AM

Page 11: [39] Deleted	LW	4/14/20 11:30:00 AM

Page 11: [39] Deleted	LW	4/14/20 11:30:00 AM

Page 11: [39] Deleted	LW	4/14/20 11:30:00 AM

Page 11: [39] Deleted	LW	4/14/20 11:30:00 AM

Page 11: [39] Deleted	LW	4/14/20 11:30:00 AM

Page 11: [40] Deleted	Yusen Yuan	4/9/20 8:06:00 PM

Page 11: [41] Formatted	Yusen Yuan	4/11/20 6:53:00 PM

Font: (Asian) +Body Asian (SimSun), Font color: Auto, Not Superscript/ Subscript

Page 11: [41] Formatted	Yusen Yuan	4/11/20 6:53:00 PM

Font: (Asian) +Body Asian (SimSun), Font color: Auto, Not Superscript/ Subscript

Page 11: [41] Formatted	Yusen Yuan	4/11/20 6:53:00 PM

Font: (Asian) +Body Asian (SimSun), Font color: Auto, Not Superscript/ Subscript

Page 11: [41] Formatted	Yusen Yuan	4/11/20 6:53:00 PM

Font: (Asian) +Body Asian (SimSun), Font color: Auto, Not Superscript/ Subscript

Page 11: [41] Formatted	Yusen Yuan	4/11/20 6:53:00 PM

Font: (Asian) +Body Asian (SimSun), Font color: Auto, Not Superscript/ Subscript

Page 11: [41] Formatted	Yusen Yuan	4/11/20 6:53:00 PM

Font: (Asian) +Body Asian (SimSun), Font color: Auto, Not Superscript/ Subscript

Page 11: [41] Formatted	Yusen Yuan	4/11/20 6:53:00 PM

Font: (Asian) +Body Asian (SimSun), Font color: Auto, Not Superscript/ Subscript

Page 11: [41] Formatted	Yusen Yuan	4/11/20 6:53:00 PM

Font: (Asian) +Body Asian (SimSun), Font color: Auto, Not Superscript/ Subscript

Page 11: [41] Formatted	Yusen Yuan	4/11/20 6:53:00 PM

Font: (Asian) +Body Asian (SimSun), Font color: Auto, Not Superscript/ Subscript

Page 11: [41] Formatted	Yusen Yuan	4/11/20 6:53:00 PM

Font: (Asian) +Body Asian (SimSun), Font color: Auto, Not Superscript/ Subscript

Page 11: [41] Formatted	Yusen Yuan	4/11/20 6:53:00 PM

Font: (Asian) +Body Asian (SimSun), Font color: Auto, Not Superscript/ Subscript

Page 11: [41] Formatted	Yusen Yuan	4/11/20 6:53:00 PM

Font: (Asian) +Body Asian (SimSun), Font color: Auto, Not Superscript/ Subscript

Page 11: [41] Formatted	Yusen Yuan	4/11/20 6:53:00 PM

Font: (Asian) +Body Asian (SimSun), Font color: Auto, Not Superscript/ Subscript

Page 11: [42] Formatted	LW	4/14/20 11:31:00 AM

Font: (Asian) +Body Asian (SimSun), Font color: Auto, Not Superscript/ Subscript

Page 11: [43] Formatted	Yusen Yuan	4/9/20 11:13:00 PM

Font: Bold

Page 11: [43] Formatted	Yusen Yuan	4/9/20 11:13:00 PM

Font: Bold

Page 11: [43] Formatted	Yusen Yuan	4/9/20 11:13:00 PM

Font: Bold

Page 11: [43] Formatted	Yusen Yuan	4/9/20 11:13:00 PM

Font: Bold

Page 11: [44] Deleted	Yusen Yuan	4/9/20 11:07:00 PM

Page 11: [44] Deleted	Yusen Yuan	4/9/20 11:07:00 PM

Page 11: [44] Deleted	Yusen Yuan	4/9/20 11:07:00 PM

Page 28: [45] Deleted	Yusen Yuan	4/9/20 6:02:00 PM